Mathematical Modelling and Control

http://www.aimspress.com/journal/mmc

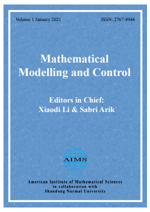

MMC, 3(4): 278–305.
DOI: 10.3934/mmc.2023024
Received: 14 December 2022
Revised: 21 February 2023
Accepted: 03 March 2023
Published: 07 December 2023

Research article

On the discontinuous dynamics of a class of 2-DOF frictional vibration systems with asymmetric elastic constraints

Wen Zhang, Jinjun Fan* **and Yuanyuan Peng**

School of Mathematics and Statistics, Shandong Normal University, Ji'nan, 250014, China

* **Correspondence:** E-mail: fjj18@126.com.

Abstract: In this paper, the discontinuous dynamic behavior of a two-degree-of-freedom frictional collision system including intermediate elastic collision and unilateral elastic constraints subjected to periodic excitation is studied by using flow switching theory. In this system, given that the motion of each object might have a velocity that is either greater than or less than zero and each object experiences a periodic excitation force that has negative feedback, because the kinetic and static friction coefficients differ, the flow barrier manifests when the object's speed is zero. Based on the discontinuity or nonsmoothness of the oscillator's motion generated by elastic collision and friction, the motion states of the oscillator in the system are divided into 16 cases and the absolute and relative coordinates are used to define various boundaries and domains in the oscillator motion's phase space. On the basis of this, the G-function and system vector fields are used to propose the oscillator motion's switching rules at the displacement and velocity boundaries. Finally, some dynamic behaviors for the 2-DOF oscillator are demonstrated via numerical simulation of the oscillator's stick, grazing, sliding and periodic motions and the scene of sliding bifurcation. The mechanical system's optimization designs with friction and elastic collision will benefit from this investigation's findings.

Keywords: flow switchability; discontinuous dynamical system; asymmetric elastic constraints; grazing motion; stick-sliding motion; flow barrier

1. Introduction

In real life, elastic collision systems with friction and clearance are widely used in mechanical systems, vehicle engineering and other fields; and, the vibro-impact system is a kind of common nonlinear dynamical system. For the parameter optimization design and service life extension of nonsmooth mechanical systems with clearance and restrictions, the study of collision and vibration is extremely important. Numerous academics have investigated vibro-impact systems to better understand their dynamic structure, which can be useful for engineering applications.

In mechanical engineering, friction is widely used in dynamic design, controlling high-precision positioning systems, transferring power or torque and decelerating high-speed rotating components. Sometimes, friction is unnecessary because friction produces noise, affects work accuracy and stability, reduces mechanical efficiency and influences the productivity of machinery and equipment. People hope to avoid the adverse factors caused by friction, to the greatest extent, so as to enhance the mechanical system's dynamic performance. In 1930, Hartog [1] analyzed nonsmooth dynamical systems impacted by viscous damping and Coulomb friction. Feeny and Moon [2] obtained that a forced oscillator's dynamics with velocity- and displacement-related Coulomb friction force could be simplified into one-dimensional mapping dynamics in some parameter ranges in 1993. Popp et al. [3] used a frictional oscillator model to study bifurcation behavior and chaotic paths under different system parameters. In the 1990s, the dynamics of multiple frictional oscillators were described by Galvanetto [4, 5]. An invariance principle that can be applied to a Coulomb friction oscillator was investigated by Alvarez et al. [6]. In 2006, Sinou et al. [7] discussed the nonlinear dynamics in a complex aircraft braking model. In 2007, Martinez and Alvarez [8] proposed a controller for a two-degree-of-freedom (2-DOF) mechanical system that has unactuated discontinuous joint friction. Through theoretical studies and experimental verification, an attempt was made to use vibration-related friction to improve the efficiency of the relevant equipment in [9]. The analytical criterion for the dry friction oscillator with SDOF (single-degree-of-freedom) stick-slip periodic solution was obtained in [10]. Fang and Jian [11] investigated the relationships among the other factors, external Coulomb dry friction and system's steady-state motion through a model of a vibration-driven system. In the same year, Liu and Wen [12] proposed a kind of controller and proved the closed-loop system's asymptotic stability by establishing an SDOF mass-spring-friction dynamical model. Based on Coulomb friction, Saadabad et al. [13] deduced and simplified the dynamic motion equation for the microrobot and obtained the causes for the stick-slip motion of the microrobot.

The collision phenomenon exists widely in various mechanical devices, and the nonlinear motion caused by a collision is the main reason for mechanical components' fatigue and structural damage. Vibro-impact systems' dynamic behavior is significantly impacted by a collision. Therefore, it is of great importance to study the impact system's dynamic behavior by combining qualitative and quantitative methods. In 1990, Balachandran and Nayfeh [14] addressed the flexible L-shaped beam-mass structure's dynamic plane response at a low excitation level. A few years later, the thin-walled structure's dynamics under impact stimulation were taken into account by Balachandran et al. [15, 16]. Two elastic balls colliding dynamically in a viscous fluid were analyzed by Zhang et al. [17]. In 2007, by applying the mechanics principle, Liu et al. [18] used the mass-spring model of dynamic cloth to describe a collision response process. In [19], a dynamic collision detection algorithm was proposed for the behaviors of the virtual battlefield. The impact dynamics characteristics of large concrete blocks were studied experimentally by Ma et al. [20]. The authors of [21] addressed the impact force performance of a vibro-impact system under various stimulation frequencies. Bichri et al. [22] analytically and numerically investigated the most reasonable method for regulating the vibro-impact dynamics of a single-sided Hertzian contact forced oscillator in 2011. The author of [23] developed and applied an enhanced single-unit vibro-impact system in their investigation. In 2018, the chaotic properties of a nonlinear energy sink system with vibration and impact were analyzed by Li et al. [24].

The degree of freedom and periodicity affect how the vibro-impact system behaves dynamically. In 1970, Harris [25] analyzed the existence of the ideal spring-mass system infinite period motion with two and multiple degrees of freedom. Campen et al. [26] discussed the periodically excited mechanical system's long-term behavior. Vorst et al. [27] examined a sophisticated multiple-degree-of-freedom (multi-DOF) beam system with an intermediate elastic stop in 1996. In [28, 29], Natsiavas and Verros examined a class of nonlinear SDOF oscillator periodic motions' stability and their dynamics. In 2002, Janin and Lamarque [30] examined an SDOF shock oscillator's stability. Arsenault and Gosselin [31] analyzed the planar 2-DOF tensegrity mechanism's dynamical model and proposed a preliminary control scheme. In 2007, sliding motion's switching conditions of forced linear oscillators with periodicity and dry friction were proposed by Luo and Gegg [32]. In addition, Luo et al. [33] employed the Poincaré map to examine the vibro-impact system's nonlinear dynamics while taking into account an n-DOF system that was subjected to periodic stimulation. In 2008, the 2-DOF dry friction oscillator's characteristics were studied by Pascal [34]. In 2012, Luo and Huang [35] discussed a nonlinear oscillator's discontinuous dynamics. Igumnov et al. [36] analyzed the dynamics of a friction system located in a rough belt. In a time-delayed, periodically driven, twin-well Duffing oscillator, Xing and Luo [37] discussed bifurcation trees with period-3 motions to chaos.

With regard to discontinuous dynamical systems, Filippov [38, 39] discussed the right-hand sides discontinuous differential equation solutions' existence and uniqueness. It is not sufficient to study the complex dynamic behavior of nonsmooth dynamical systems only by applying Filippov's theory. To explore the flow's local singularity closer to the separation boundary in more detail through the use of connectable and accessible sub-domains, a local theory of nonsmooth dynamical systems is explored by Luo [40]. Luo and Gegg [41] investigated the periodic motion of a vibrator moving in a periodic vibration band with dry friction and gave the grazing and stick bifurcations in the same year. Under the condition of flow barriers existing in discontinuous dynamic systems, the condition of flow passing through a separation boundary was studied by Luo [42]. In addition, by using the set-valued vector field theory, Luo [43] has provided the sliding motion's switching conditions on the separation boundary. In [44], the G-function was designed to study discontinuous dynamical systems' singularity. In 2009, Luo [45] clearly described the dynamic regions' discontinuous dynamical system theory. The analytical parameters of sliding flow and nonsliding flow at the velocity boundary were reported in [46]. Luo [47] systematically elaborated the flow switching theory in 2010. The flow barrier theory was established by Luo [48] for discontinuous dynamical systems. Currently, a growing number of academics are starting to explore several dynamical systems by using the flow switching theory. In 2015, Fu and Zhang [49] investigated inclined impact oscillator's behavior with periodic excitation. In 2017, based on the local theory of flow at the corner in discontinuous dynamical systems, the analytical criteria for switching impact-alike chatter at corners were discovered by Huang and Luo [50]. Fan et al. [51] looked into a switching control law-based friction-induced oscillator. [52–54] explored the 2-DOF friction oscillators' motion switching conditions on the separation boundary. In addition, more and more scholars are studying the bifurcation characteristics of dynamical systems; for instance, Li et al. [55] investigated various sliding bifurcations by using the discontinuous predator-prey model in 2021.

However, more needs to be said about the local singularity created at the separation boundary of some dynamical systems. In this research, an in-depth study of the dynamic behavior of a class of 2-DOF frictional vibration systems with asymmetric elastic constraints is conducted. Compared with the physical models studied previously, the model studied in this paper considers the following factors: (i) negative feedback that makes the system more stable; (ii) simultaneous occurrence of left and right elastic collisions; (iii) flow barriers existing at velocity boundaries, which results in more complex conditions for the disappearance of sliding motion.

The study of the model discussed in this paper differs from the research on the vibro-impact models in earlier studies, and the motion switching on the separation boundary for this kind of system has not yet been thoroughly researched. We will give the switching criteria for an oscillator at the separation boundaries. Moreover, we provide numerical simulations for some typical motions and the sliding bifurcation scene in order to vividly show the diversity and complexity of the oscillator's motion. The motion states of objects become more strongly connected and the corresponding boundaries and domains become more time-dependent as the degrees of freedom and number of discontinuous factors increase; thus, we investigate the 2-DOF system by using the approach of first individually studying each object in the system before combining them to analyze the behavior of the entire system.

At present, there are relatively few studies on the application of the flow switchability theory to the 2-DOF system in which the elastic impact on the left and right sides may occur simultaneously; this paper enriches this theory. This kind of elastic collision system is close to what occurs in practical engineering applications. The study serves as an original and deep investigation into the discontinuous dynamics of a class of 2-DOF frictional vibration systems with asymmetric elastic constraints through the application of strict mathematical consideration, which can deepen the understanding of machine collision-related systems and is beneficial to improve the stability and the service life of machines.

The article has the following structure. The physical model of a 2-DOF frictional vibration system with asymmetric elastic restrictions is introduced, and the system's various motion states are listed in Section 3. In Section 4, the domain and boundary of the oscillators are divided by using the absolute and relative phase spaces associated with the discontinuity or nonsmoothness of the system, and the vector equation in each domain is obtained. In Section 5, the flow switchability theory and flow barrier theory are used to present the analytical criteria for the motion switching at the separation boundary. Additionally, numerical simulations are presented to demonstrate the analytical criteria in Section 6. Section 7 depicts the scene of sliding bifurcation as the excitation frequency and amplitude change. The entire article is summarized at the end in Section 8.

2. Explanation of symbols

For a clearer understanding of the content of this article, Table 1 summarizes the definitions of the symbols used in this paper.

Table 1. Symbols used in this paper.

Symbols	Description
K_1, K_3, K_4, K_6	Linear spring
K_2, K_5	Nonlinear spring
C_1, C_3, C_4	Linear damping
C_2, C_5	Nonlinear damping
d_1	Distance of linear spring K_6 and mass m_1's equilibrium position
d	Distance of linear spring-damping (K_3, C_3) and mass m_1's equilibrium position
x_i	Object m_i's $(i \in \{1,2\})$ horizontal displacement
$\dot{x}_i$	Object m_i's $(i \in \{1,2\})$ velocity
$\ddot{x}_i$	Object m_i's $(i \in \{1,2\})$ accelerated velocity
F_i	Periodic force acting on object m_i $(i \in \{1,2\})$
Q_i	Excitation amplitude of object m_i $(i \in \{1,2\})$
Ω	Frequency
φ_i	Initial phase of object m_i $(i \in \{1,2\})$
P_i	Positive constant force of object m_i $(i \in \{1,2\})$
B_i	Negative feedback of object m_i $(i \in \{1,2\})$
μ_k	Kinetic friction coefficient
μ_s	Static friction coefficient
$F_N^{(i)}$	Normal force acting on object m_i $(i \in \{1,2\})$
g	Acceleration of gravity
$-F_f^{(i)}$	Friction force acting on object m_i $(i \in \{1,2\})$
q_i	Excitation amplitude of per unit mass of object m_i $(i \in \{1,2\})$
p_i	Positive constant force of per unit mass of object m_i $(i \in \{1,2\})$
b_i	Negative feedback of per unit mass of object m_i $(i \in \{1,2\})$
$-f^{(i)}$	Friction force of per unit mass acting on object m_i $(i \in \{1,2\})$
$c_\theta^{(i)}$ $(\theta = 1, \cdots, 5)$	Damping of stiffness coefficient per unit mass
$k_\sigma^{(i)}$ $(\sigma = 1, \cdots, 6)$	Spring of stiffness coefficient per unit mass
$F_s^{(i)}$	Non-friction force affecting object m_i $(i \in \{1,2\})$
$\Omega^{(i)}$	Mass m_i's $(\in \{1,2\})$ motion domain
$\partial\Omega^{(i)}$	Mass m_i's $(i \in \{1,2\})$ boundary
$\varphi^{(i)}$	Constraint function on boundary $\partial\Omega^{(i)}$
δ_i	Mass m_i's $(i \in \{1,2\})$ motion domain or boundary
$\mathbf{x}_i^{(\delta_i)}$	Mass m_i's $(i \in \{1,2\})$ state vector in absolute coordinates
$\dot{\mathbf{x}}_i^{(\delta_i)}$	Derivative of mass m_i's $(i \in \{1,2\})$ state vector in absolute coordinates
$\mathbf{F}_i^{(\delta_i)}, \mathbf{H}_i^{(\delta_i)}$	Vector field for mass m_i $(i \in \{1,2\})$ in absolute coordinates
z_i	Relative displacement
$\dot{z}_i$	Relative velocity
$\ddot{z}_i$	Relative accelerated velocity
$\mathbf{z}_1^{(\delta_1)}$	Mass m_1's state vector in relative coordinates
$\dot{\mathbf{z}}_1^{(\delta_1)}$	Derivative of mass m_1's state vector in relative coordinates
$\mathbf{K}_1^{(\delta_1)}, \mathbf{S}_1^{(\delta_1)}$	Vector field for mass m_1 in relative coordinates
δ	Mass m_i's $(i \in \{1,2\})$ δ-side domain
$\mathbf{F}_i^{(0>0_\delta)}$, $\mathbf{H}_i^{(0>0_\delta)}$	Flow barrier vector fields on δ-side of velocity boundary in absolute coordinates
$f_{si}^{(\delta)}$	Static friction force per unit of mass exerting on δ-side of velocity boundary on mass m_i $(i \in \{1,2\})$
$\mathbf{n}_{\partial\Omega_{ln}^{(1)}}$	Normal vectors of displacement boundary $\partial\Omega_{ln}^{(1)}$
$\mathbf{n}_{\partial\Omega_{\alpha\beta}^{(i)}}$	Normal vectors of velocity boundary $\partial\Omega_{\alpha\beta}^{(i)}$ $(i \in \{1,2\})$
$G_{\partial\Omega_{\alpha\beta}^{(i)}}^{(0,\delta)}$	0th-order G-function on velocity boundary $\partial\Omega_{\alpha\beta}^{(i)}$ $(i \in \{1,2\})$
$G_{\partial\Omega_{\alpha\beta}^{(i)}}^{(1,\delta)}$	1st-order G-function on velocity boundary $\partial\Omega_{\alpha\beta}^{(i)}$ $(i \in \{1,2\})$
$G_{\partial\Omega_{ln}^{(1)}}^{(0,\delta)}$	0th-order G-function on isplacement boundary $\partial\Omega_{ln}^{(1)}$
$G_{\partial\Omega_{ln}^{(1)}}^{(1,\delta)}$	1st-order G-function on displacement boundary $\partial\Omega_{ln}^{(1)}$
$D\mathbf{F}_i^{(\delta)}$	Derivative of $\mathbf{F}_i^{(\delta)}$ $(i \in \{1,2\})$ in absolute coordinates
$D\mathbf{H}_i^{(\delta)}$	Derivative of $\mathbf{H}_i^{(\delta)}$ $(i \in \{1,2\})$ in absolute coordinates
$G_{\partial\Omega_{\alpha\beta}^{(i)}}^{(0,0>0_\delta)}$	0th-order G-function with flow barrier on velocity boundary $\partial\Omega_{\alpha\beta}^{(i)}$ $(i \in \{1,2\})$
$G_{\partial\Omega_{\alpha\beta}^{(i)}}^{(1,0>0_\delta)}$	1st-order G-function with flow barrier on velocity boundary $\partial\Omega_{\alpha\beta}^{(i)}$ $(i \in \{1,2\})$
$D\mathbf{F}_i^{(0>0_\delta)}$	Derivative of $\mathbf{F}_i^{(0>0_\delta)}$ $(i \in \{1,2\})$ in absolute coordinates
$D\mathbf{H}_i^{(0>0_\delta)}$	Derivative of $\mathbf{H}_i^{(0>0_\delta)}$ $(i \in \{1,2\})$ in absolute coordinates
$D\mathbf{K}_1^{(\delta)}$	Derivative of $\mathbf{K}_1^{(\delta)}$ in relative coordinates
$D\mathbf{S}_1^{(\delta)}$	Derivative of $\mathbf{S}_1^{(\delta)}$ in relative coordinates

3. Dynamical model

3.1. Physical model

A 2-DOF frictional vibration system with asymmetric elastic constraints is depicted in Figure 1, and it mainly consists of two masses m_1 and m_2. A variable spring with stiffness coefficients K_1 and K_2, as well as a variable damper with stiffness coefficients C_1 and C_2, are used to attach the mass m_1 to the right vertical wall, and the distance between the linear spring with stiffness coefficient K_6 and the mass m_1's equilibrium position is d_1. A variable spring with stiffness coefficients of K_4 and K_5, as well as a variable damper with stiffness coefficients of C_4 and C_5, are used to attach the mass m_2 to the left vertical wall.

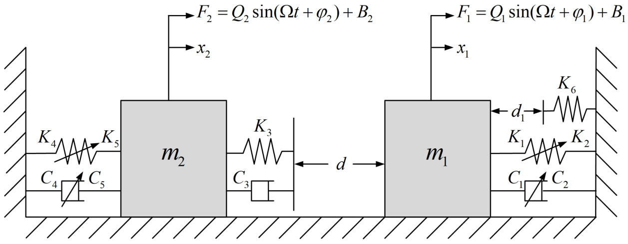

Figure 1. Physical model.

In addition, there is an elastic constraint connected to the right end of the mass m_2, where this constraint is made up of a linear damper C_3 and a linear spring K_3, and this constraint's distance from the mass m_1 is d when both the object m_1 and the object m_2 are in the equilibrium position. In the physical model, springs K_2 and K_5 and dampers C_2 and C_5 are nonlinear spring-dampers cubic term. When converting potential energy, the nonlinear spring-damper exhibits little deformation, which is conducive to regulating the motion of mechanical parts, mitigating collision or vibration and storing energy.

The nonlinear spring-damper model is widely utilized as a shock absorber in construction, machinery, aerospace and other areas because it can precisely reflect the energy loss during collision processes. x_1 and x_2 respectively represent the object m_1's and the object m_2's horizontal displacements; and, the mass m_i ($i \in \{1,2\}$) is motivated by the periodic force $F_i = Q_i\sin(\Omega t + \varphi_i) + B_i$, with the negative feedback

$$B_i \triangleq B_i(\dot{x}_i) = \begin{cases} -P_i, & \dot{x}_i > 0, \\ 0, & \dot{x}_i = 0, \\ P_i, & \dot{x}_i < 0, \end{cases} \tag{3.1}$$

where Q_i and P_i are the excitation amplitude and positive constant force, respectively, Ω is the frequency, φ_i is the initial phase and the mass m_i's velocity is $\dot{x}_i = dx_i/dt$.

Figure 2 illustrates the friction model; the kinetic friction coefficient is μ_k and μ_s is the static friction coefficient, where the friction force between the mass m_i ($i \in \{1,2\}$) and the ground is defined as

$$F_f^{(i)} \begin{cases} = -\mu_k F_N^{(i)}, & \dot{x}_i < 0, \\ \in [-\mu_s F_N^{(i)}, \mu_s F_N^{(i)}], & \dot{x}_i = 0, \\ = \mu_k F_N^{(i)}, & \dot{x}_i > 0, \end{cases} \tag{3.2}$$

where $F_N^{(i)}$ ($F_N^{(i)} = m_i g$, g is the acceleration of gravity) is the normal force acting on the object m_i ($i \in \{1,2\}$). In addition, the static friction force ranges from $[-\mu_s F_N^{(i)}, \mu_s F_N^{(i)}]$.

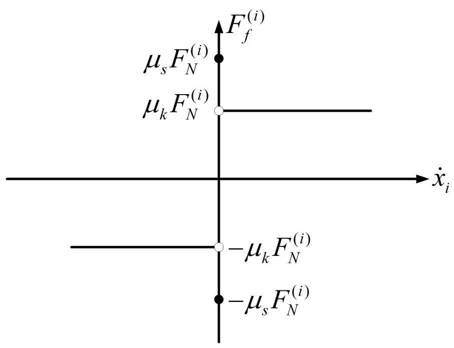

Figure 2. Friction force between the mass m_i ($i \in \{1,2\}$) and the ground.

3.2. Analysis of oscillator's motion

The following notations are given for convenience:

$$\begin{aligned} & q_i = \frac{Q_i}{m_i}, \ b_i \triangleq b_i(\dot{x}_i) = \frac{B_i}{m_i}, \ p_i = \frac{P_i}{m_i}, \\ & f^{(i)} = \frac{F_f^{(i)}}{m_i}, \ c_\theta^{(i)} = \frac{C_\theta^{(i)}}{m_i} (\theta = 1,2,3,4,5), \\ & k_\sigma^{(i)} = \frac{K_\sigma^{(i)}}{m_i} (\sigma = 1,2,3,4,5,6), \end{aligned} \tag{3.3}$$

where $i = 1, 2$.

Based on whether the object m_1 touches the constraint (K_3, C_3) on the left or the constraint (K_6) on the right, we can easily obtain the non-friction forces $F_s^{(1)}$ and $F_s^{(2)}$ affecting the objects m_1 and m_2, respectively; and, the expressions of $F_s^{(1)}$ and $F_s^{(2)}$ are as follows:

$$F_s^{(1)} = \begin{cases} Q_1 \sin(\Omega t + \varphi_1) + B_1 - K_1 x_1 - K_2 (x_1)^3 \\ \quad -C_1 \dot{x}_1 - C_2 (\dot{x}_1)^3, \quad \text{if } x_1 - x_2 > -d \text{ and } x_1 < d_1; \\ Q_1 \sin(\Omega t + \varphi_1) + B_1 - K_1 x_1 - K_2 (x_1)^3 \\ \quad -C_1 \dot{x}_1 - C_2 (\dot{x}_1)^3 - K_3 (x_1 - x_2 + d) \\ \quad -C_3 (\dot{x}_1 - \dot{x}_2), \quad \text{if } x_1 - x_2 \leqslant -d \text{ and } x_1 < d_1; \\ Q_1 \sin(\Omega t + \varphi_1) + B_1 - K_1 x_1 - K_2 (x_1)^3 \\ \quad -C_1 \dot{x}_1 - C_2 (\dot{x}_1)^3 \\ \quad -K_6 (x_1 - d_1), \quad \text{if } x_1 - x_2 > -d \text{ and } x_1 \geqslant d_1; \\ Q_1 \sin(\Omega t + \varphi_1) + B_1 - K_1 x_1 - K_2 (x_1)^3 \\ \quad -C_1 \dot{x}_1 - C_2 (\dot{x}_1)^3 - K_6 (x_1 - d_1) \\ \quad -C_3 (\dot{x}_1 - \dot{x}_2) \\ \quad -K_3 (x_1 - x_2 + d), \quad \text{if } x_1 - x_2 \leqslant -d \text{ and } x_1 \geqslant d_1, \end{cases} \tag{3.4}$$

$$F_s^{(2)} = \begin{cases} Q_2 \sin(\Omega t + \varphi_2) + B_2 - K_4 x_2 - K_5 (x_2)^3 \\ \quad -C_4 \dot{x}_2 - C_5 (\dot{x}_2)^3, \ \text{if } x_1 - x_2 > -d; \\ Q_2 \sin(\Omega t + \varphi_2) + B_2 - K_4 x_2 - K_5 (x_2)^3 \\ \quad -C_4 \dot{x}_2 - C_5 (\dot{x}_2)^3 - K_3 (x_2 - x_1 - d) \\ \quad -C_3 (\dot{x}_2 - \dot{x}_1), \quad \text{if } x_1 - x_2 \leqslant -d. \end{cases} \tag{3.5}$$

According to the above discussion, the 2-DOF frictional vibration system with asymmetric elastic constraints has 16 states of motion, which are listed below.

(i) When the object m_1 and the object m_2 are not interacting (i.e., $x_1 - x_2 > -d$) and the object m_1 is not touching the right elastic constraint K_6 (i.e., $x_1 < d_1$), the system has four states of motion: i.e., $\dot{x}_1 \neq 0, \dot{x}_2 \neq 0$ (the object m_1's free-flight motion or nonsliding motion and the object m_2's free-flight motion or nonsliding motion); $\dot{x}_1 = 0, \dot{x}_2 \neq 0$ (the object m_1's sliding motion and the object m_2's free-flight motion or nonsliding motion); $\dot{x}_1 \neq 0, \dot{x}_2 = 0$ (the object m_1's free-flight motion or nonsliding motion and the object m_2's sliding motion); or $\dot{x}_1 = 0, \dot{x}_2 = 0$ (the object m_1's sliding motion and the object m_2's sliding motion).

(ii) When the object m_1 and the object m_2 are not interacting (i.e., $x_1 - x_2 > -d$) and the right elastic constraint K_6 is touched by the object m_1 (i.e., $x_1 \geq d_1$), the system has four states of motion: i.e., $\dot{x}_1 \neq 0, \dot{x}_2 \neq 0$ (the object m_1's right stick-nonsliding motion and the object m_2's free-flight motion or nonsliding motion); $\dot{x}_1 = 0, \dot{x}_2 \neq 0$ (the object m_1's right stick-sliding motion and the object m_2's free-flight motion or nonsliding motion); $\dot{x}_1 \neq 0, \dot{x}_2 = 0$ (the object m_1's right stick-nonsliding motion and the object m_2's sliding motion); or $\dot{x}_1 = 0, \dot{x}_2 = 0$ (the object m_1's right stick-sliding motion and the object m_2's sliding motion).

(iii) When the object m_1 is interacting with the object m_2 (i.e., $x_1 - x_2 \leqslant -d$) and the object m_1 is not touching the right elastic constraint K_6 (i.e., $x_1 < d_1$), the system has four states of motion: i.e., $\dot{x}_1 \neq 0, \dot{x}_2 \neq 0$ (the object m_1's left stick-nonsliding motion and the object m_2's stick-nonsliding motion); $\dot{x}_1 = 0, \dot{x}_2 \neq 0$ (the object m_1's left stick-sliding motion and the object m_2's stick-nonsliding motion); $\dot{x}_1 \neq 0, \dot{x}_2 = 0$ (the object m_1's left stick-nonsliding motion and the object m_2's stick-sliding motion); or $\dot{x}_1 = 0, \dot{x}_2 = 0$ (the object m_1's left stick-sliding motion and the object m_2's stick-sliding motion).

(iv) When the object m_1 is interacting with the object m_2 (i.e., $x_1 - x_2 \leqslant -d$) and the right elastic constraint K_6 is touched by the object m_1 (i.e., $x_1 \geq d_1$), the system has four states of motion: i.e., $\dot{x}_1 \neq 0, \dot{x}_2 \neq 0$ (the object m_1's double stick-nonsliding motion and the object m_2's stick-nonsliding motion); $\dot{x}_1 = 0, \dot{x}_2 \neq 0$ (the object m_1's double stick-sliding motion and the object m_2's stick-nonsliding motion); $\dot{x}_1 \neq 0, \dot{x}_2 = 0$ (the object m_1's double stick-nonsliding motion and the object m_2's stick-sliding motion); or $\dot{x}_1 = 0, \dot{x}_2 = 0$ (the object m_1's double stick-sliding motion and the object m_2's stick-sliding motion).

4. Phase space partition and vector equations

The oscillator's motion in the 2-DOF dynamic system is complex and discontinuous because of dry friction, the unequal coefficients of static/dynamic friction and elastic impacts. With the purpose of conducting a more thorough analysis of the separation boundary's motion switching issue in this discontinuous dynamical system, the domains and boundaries shall be initially defined in absolute and relative coordinates, respectively, so that two objects maintain continuous motion in each domain; then, by introducing vector fields of the two objects in the phase space, the two object's motion equations can be expressed as vectors.

4.1. Phase space partition

According to whether the mass m_1 makes the left stick motion (i.e., whether the mass m_2 makes the stick motion), the oscillator's motion in phase space has the following domain and boundary division.

Case I: Without left stick motion for the mass m_1.

The mass m_1's four domains are represented as

$$\begin{cases} \Omega_1^{(1)} = \{(x_1, \dot{x}_1) \mid x_1 < d_1,\ x_1 - x_2 > -d,\ \dot{x}_1 > 0\}, \\ \Omega_2^{(1)} = \{(x_1, \dot{x}_1) \mid x_1 < d_1,\ x_1 - x_2 > -d,\ \dot{x}_1 < 0\}, \\ \Omega_3^{(1)} = \{(x_1, \dot{x}_1) \mid x_1 > d_1,\ x_1 - x_2 > -d,\ \dot{x}_1 > 0\}, \\ \Omega_4^{(1)} = \{(x_1, \dot{x}_1) \mid x_1 > d_1,\ x_1 - x_2 > -d,\ \dot{x}_1 < 0\}, \end{cases} \tag{4.1}$$

and the associated boundaries are described as

$$\begin{cases} \partial\Omega_{12}^{(1)} = \partial\Omega_{21}^{(1)} = \{(x_1, \dot{x}_1) \mid \varphi_{12}^{(1)} = \varphi_{21}^{(1)} \equiv \dot{x}_1 = 0,\ x_1 < d_1, \\ \qquad x_1 - x_2 > -d\}, \\ \partial\Omega_{34}^{(1)} = \partial\Omega_{43}^{(1)} = \{(x_1, \dot{x}_1) \mid \varphi_{34}^{(1)} = \varphi_{43}^{(1)} \equiv \dot{x}_1 = 0,\ x_1 > d_1, \\ \qquad x_1 - x_2 > -d\}, \\ \partial\Omega_{13}^{(1)} = \partial\Omega_{31}^{(1)} = \{(x_1, \dot{x}_1) \mid \varphi_{13}^{(1)} = \varphi_{31}^{(1)} \equiv x_1 - d_1 = 0, \\ \qquad x_1 - x_2 > -d,\ \dot{x}_1 > 0\}, \\ \partial\Omega_{24}^{(1)} = \partial\Omega_{42}^{(1)} = \{(x_1, \dot{x}_1) \mid \varphi_{24}^{(1)} = \varphi_{42}^{(1)} \equiv x_1 - d_1 = 0, \\ \qquad x_1 - x_2 > -d,\ \dot{x}_1 < 0\}, \\ \partial\Omega_{1\infty}^{(1)} = \{(x_1, \dot{x}_1) \mid \varphi_{1\infty}^{(1)} \equiv x_1 - x_2 + d = 0,\ x_1 < d_1,\ \dot{x}_1 > 0\}, \\ \partial\Omega_{2\infty}^{(1)} = \{(x_1, \dot{x}_1) \mid \varphi_{2\infty}^{(1)} \equiv x_1 - x_2 + d = 0,\ x_1 < d_1,\ \dot{x}_1 < 0\}. \end{cases} \tag{4.2}$$

Figure 3a represents the mass m_1's above domains and boundaries. The domains $\Omega_1^{(1)}$ and $\Omega_2^{(1)}$ indicate the free-flight domains, which are symbolized by yellow and light blue, respectively; the right stick domains $\Omega_3^{(1)}$ and $\Omega_4^{(1)}$ are represented by purple and orange, respectively; the black dashed line and black dotted line are used to depict the velocity boundaries $\partial\Omega_{12}^{(1)}$ and $\partial\Omega_{34}^{(1)}$, respectively; red dashed lines signify the right stick displacement boundaries $\partial\Omega_{13}^{(1)}$ and $\partial\Omega_{24}^{(1)}$; and, the permanent boundary $\partial\Omega_{i\infty}^{(1)}$ ($i \in \{1, 2\}$) is represented by the pink dashed curve.

The two domains of the mass m_2 are expressed as

$$\begin{cases} \Omega_1^{(2)} = \{(x_2, \dot{x}_2) \mid x_1 - x_2 > -d,\ \dot{x}_2 < 0\}, \\ \Omega_2^{(2)} = \{(x_2, \dot{x}_2) \mid x_1 - x_2 > -d,\ \dot{x}_2 > 0\}, \end{cases} \tag{4.3}$$

and the associated boundaries are specified as

$$\begin{cases} \partial\Omega_{1\infty}^{(2)} = \{(x_2, \dot{x}_2) \mid \varphi_{1\infty}^{(2)} \equiv x_1 - x_2 + d = 0, \\ \qquad \dot{x}_2 < 0\}, \\ \partial\Omega_{2\infty}^{(2)} = \{(x_2, \dot{x}_2) \mid \varphi_{2\infty}^{(2)} \equiv x_1 - x_2 + d = 0, \\ \qquad \dot{x}_2 > 0\}, \\ \partial\Omega_{12}^{(2)} = \partial\Omega_{21}^{(2)} = \{(x_2, \dot{x}_2) \mid \varphi_{12}^{(2)} = \varphi_{21}^{(2)} \equiv \dot{x}_2 = 0, \\ \qquad x_1 - x_2 > -d\}. \end{cases} \tag{4.4}$$

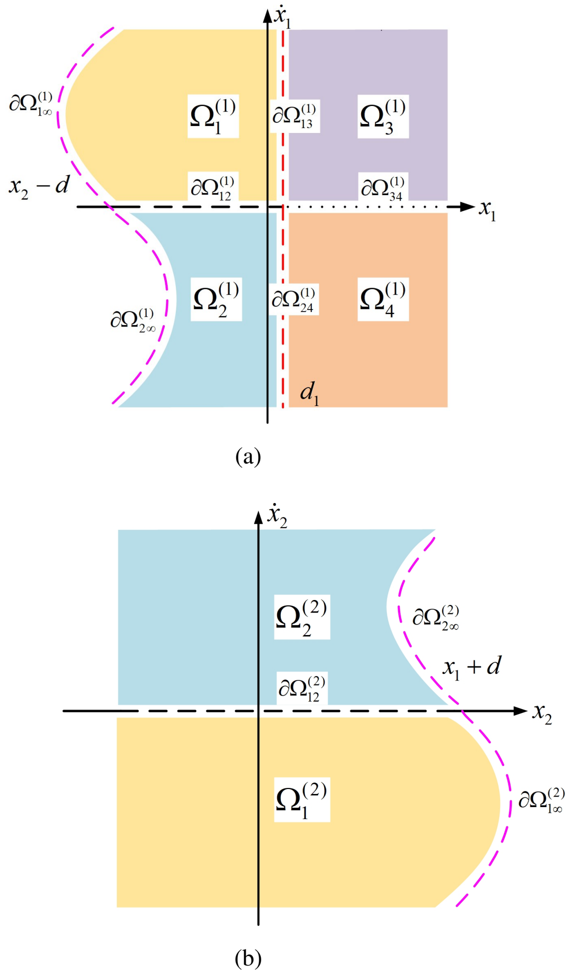

Figure 3. Domain and boundary division in absolute coordinates: (a) without left stick motion for the mass m_1; (b) without stick motion for the mass m_2.

In this case, Figure 3b represents the mass m_2's above domains and boundaries. The domains $\Omega_1^{(2)}$ and $\Omega_2^{(2)}$ indicate the free-flight domains, which are shown by yellow and light blue, respectively; the black dashed line designates the velocity boundary, which is $\partial\Omega_{12}^{(2)}$; and, the permanent boundary is represented by the pink dashed line, which is $\partial\Omega_{i\infty}^{(2)}$ ($i \in \{1, 2\}$).

Case II: With left stick motion for the mass m_1.

The mass m_1's eight domains are expressed as

$$\begin{cases} \Omega_1^{(1)} = \{(x_1, \dot{x}_1) \mid x_1 < d_1,\ x_1 - x_2 > -d,\ \dot{x}_1 > 0\}, \\ \Omega_2^{(1)} = \{(x_1, \dot{x}_1) \mid x_1 < d_1,\ x_1 - x_2 > -d,\ \dot{x}_1 < 0\}, \\ \Omega_3^{(1)} = \{(x_1, \dot{x}_1) \mid x_1 > d_1,\ x_1 - x_2 > -d,\ \dot{x}_1 > 0\}, \\ \Omega_4^{(1)} = \{(x_1, \dot{x}_1) \mid x_1 > d_1,\ x_1 - x_2 > -d,\ \dot{x}_1 < 0\}, \\ \Omega_5^{(1)} = \{(x_1, \dot{x}_1) \mid x_1 < d_1,\ x_1 - x_2 < -d,\ \dot{x}_1 > 0\}, \\ \Omega_6^{(1)} = \{(x_1, \dot{x}_1) \mid x_1 < d_1,\ x_1 - x_2 < -d,\ \dot{x}_1 < 0\}, \\ \Omega_7^{(1)} = \{(x_1, \dot{x}_1) \mid x_1 > d_1,\ x_1 - x_2 < -d,\ \dot{x}_1 > 0\}, \\ \Omega_8^{(1)} = \{(x_1, \dot{x}_1) \mid x_1 > d_1,\ x_1 - x_2 < -d,\ \dot{x}_1 < 0\}, \end{cases} \tag{4.5}$$

and the associated boundaries are characterized as

$$\begin{cases} \partial\Omega_{34}^{(1)} = \partial\Omega_{43}^{(1)} = \{(x_1, \dot{x}_1) \mid \varphi_{34}^{(1)} = \varphi_{43}^{(1)} \equiv \dot{x}_1 = 0,\ x_1 > d_1, \\ \qquad x_1 - x_2 > -d\}, \\ \partial\Omega_{56}^{(1)} = \partial\Omega_{65}^{(1)} = \{(x_1, \dot{x}_1) \mid \varphi_{56}^{(1)} = \varphi_{65}^{(1)} \equiv \dot{x}_1 = 0,\ x_1 < d_1, \\ \qquad x_1 - x_2 < -d\}, \\ \partial\Omega_{78}^{(1)} = \partial\Omega_{87}^{(1)} = \{(x_1, \dot{x}_1) \mid \varphi_{78}^{(1)} = \varphi_{87}^{(1)} \equiv \dot{x}_1 = 0,\ x_1 > d_1, \\ \qquad x_1 - x_2 < -d\}, \\ \partial\Omega_{15}^{(1)} = \partial\Omega_{51}^{(1)} = \{(x_1, \dot{x}_1) \mid \varphi_{15}^{(1)} = \varphi_{51}^{(1)} \equiv x_1 - x_2 + d = 0, \\ \qquad x_1 < d_1,\ \dot{x}_1 > 0\}, \\ \partial\Omega_{26}^{(1)} = \partial\Omega_{62}^{(1)} = \{(x_1, \dot{x}_1) \mid \varphi_{26}^{(1)} = \varphi_{62}^{(1)} \equiv x_1 - x_2 + d = 0, \\ \qquad x_1 < d_1,\ \dot{x}_1 < 0\}, \\ \partial\Omega_{37}^{(1)} = \partial\Omega_{73}^{(1)} = \{(x_1, \dot{x}_1) \mid \varphi_{37}^{(1)} = \varphi_{73}^{(1)} \equiv x_1 - x_2 + d = 0, \\ \qquad x_1 > d_1,\ \dot{x}_1 > 0\}, \\ \partial\Omega_{48}^{(1)} = \partial\Omega_{84}^{(1)} = \{(x_1, \dot{x}_1) \mid \varphi_{48}^{(1)} = \varphi_{84}^{(1)} \equiv x_1 - x_2 + d = 0, \\ \qquad x_1 > d_1,\ \dot{x}_1 < 0\}, \\ \partial\Omega_{13}^{(1)} = \partial\Omega_{31}^{(1)} = \{(x_1, \dot{x}_1) \mid \varphi_{13}^{(1)} = \varphi_{31}^{(1)} \equiv x_1 - d_1 = 0, \\ \qquad x_1 - x_2 > -d,\ \dot{x}_1 > 0\}, \\ \partial\Omega_{24}^{(1)} = \partial\Omega_{42}^{(1)} = \{(x_1, \dot{x}_1) \mid \varphi_{24}^{(1)} = \varphi_{42}^{(1)} \equiv x_1 - d_1 = 0, \\ \qquad x_1 - x_2 > -d,\ \dot{x}_1 < 0\}, \\ \partial\Omega_{57}^{(1)} = \partial\Omega_{75}^{(1)} = \{(x_1, \dot{x}_1) \mid \varphi_{57}^{(1)} = \varphi_{75}^{(1)} \equiv x_1 - d_1 = 0, \\ \qquad x_1 - x_2 < -d,\ \dot{x}_1 > 0\}, \\ \partial\Omega_{68}^{(1)} = \partial\Omega_{86}^{(1)} = \{(x_1, \dot{x}_1) \mid \varphi_{68}^{(1)} = \varphi_{86}^{(1)} \equiv x_1 - d_1 = 0, \\ \qquad x_1 - x_2 < -d,\ \dot{x}_1 < 0\}. \end{cases} \tag{4.6}$$

Figure 4a represents the mass m_1's above domains and boundaries. The free-flight domains are represented by the domains $\Omega_1^{(1)}$ and $\Omega_2^{(1)}$, which are symbolized by yellow and light blue, respectively; purple and orange respectively represent the right stick domains $\Omega_3^{(1)}$ and $\Omega_4^{(1)}$; the left stick domains $\Omega_5^{(1)}$ and $\Omega_6^{(1)}$ are represented by pink and green, respectively; dark blue and gray respectively represent the double stick domains $\Omega_7^{(1)}$ and $\Omega_8^{(1)}$; the velocity boundaries $\partial\Omega_{56}^{(1)}$, $\partial\Omega_{34}^{(1)}$ and $\partial\Omega_{78}^{(1)}$ are depicted by a black dotted-dashed line, black dotted line and orange dashed line, respectively; pink dashed lines denote the left stick displacement boundaries $\partial\Omega_{15}^{(1)}$, $\partial\Omega_{37}^{(1)}$, $\partial\Omega_{48}^{(1)}$ and $\partial\Omega_{26}^{(1)}$; and, red dashed lines denote the right stick displacement boundaries $\partial\Omega_{13}^{(1)}$, $\partial\Omega_{57}^{(1)}$, $\partial\Omega_{68}^{(1)}$ and $\partial\Omega_{24}^{(1)}$.

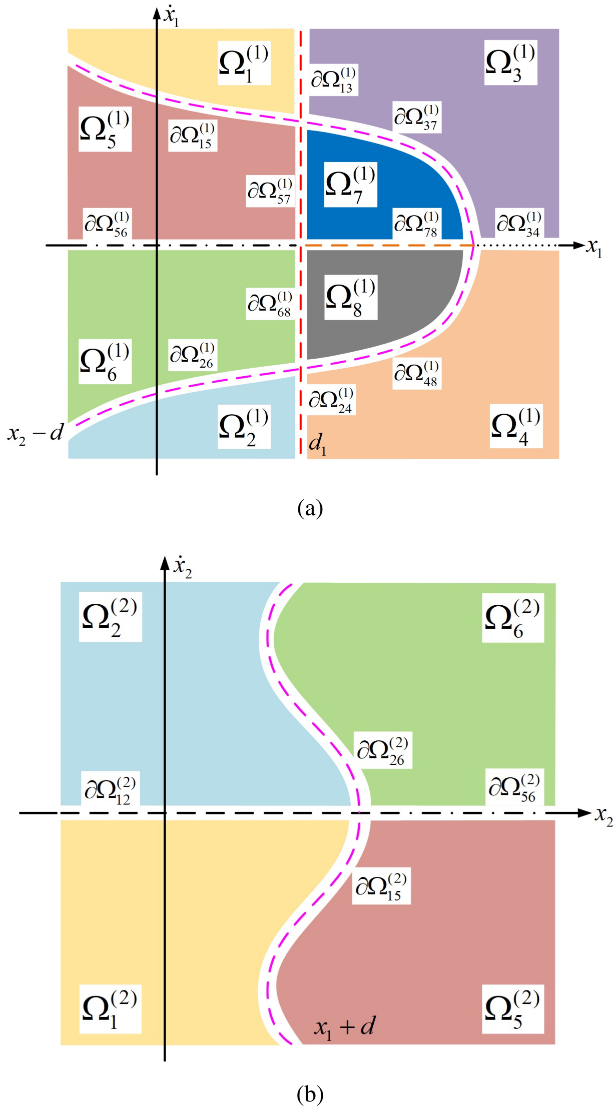

Figure 4. Domain and boundary division in absolute coordinates: (a) with left stick motion for the mass m_1; (b) with stick motion for the mass m_2.

The mass m_2's four domains are represented as

$$\begin{cases} \Omega_1^{(2)} = \{(x_2, \dot{x}_2) \mid x_1 - x_2 > -d,\ \dot{x}_2 < 0\}, \\ \Omega_2^{(2)} = \{(x_2, \dot{x}_2) \mid x_1 - x_2 > -d,\ \dot{x}_2 > 0\}, \\ \Omega_5^{(2)} = \{(x_2, \dot{x}_2) \mid x_1 - x_2 < -d,\ \dot{x}_2 < 0\}, \\ \Omega_6^{(2)} = \{(x_2, \dot{x}_2) \mid x_1 - x_2 < -d,\ \dot{x}_2 > 0\}, \end{cases} \tag{4.7}$$

and the corresponding boundaries are characterized as

$$\begin{cases} \partial\Omega_{12}^{(2)} = \partial\Omega_{21}^{(2)} = \{(x_2, \dot{x}_2) \mid \varphi_{12}^{(2)} = \varphi_{21}^{(2)} \equiv \dot{x}_2 = 0, \\ \qquad x_1 - x_2 > -d\}, \\ \partial\Omega_{56}^{(2)} = \partial\Omega_{65}^{(2)} = \{(x_2, \dot{x}_2) \mid \varphi_{56}^{(2)} = \varphi_{65}^{(2)} \equiv \dot{x}_2 = 0, \\ \qquad x_1 - x_2 < -d\}, \\ \partial\Omega_{15}^{(2)} = \partial\Omega_{51}^{(2)} = \{(x_2, \dot{x}_2) \mid \varphi_{15}^{(2)} = \varphi_{51}^{(2)} \equiv x_1 - x_2 + d = 0, \\ \qquad \dot{x}_2 < 0\}, \\ \partial\Omega_{26}^{(2)} = \partial\Omega_{62}^{(2)} = \{(x_2, \dot{x}_2) \mid \varphi_{26}^{(2)} = \varphi_{62}^{(2)} \equiv x_1 - x_2 + d = 0, \\ \qquad \dot{x}_2 > 0\}. \end{cases} \tag{4.8}$$

Figure 4b displays the mass m_2's above domains and boundaries. The domains $\Omega_1^{(2)}$ and $\Omega_2^{(2)}$ indicate the free-flight domains, which are symbolized by yellow and light blue, respectively; the domains $\Omega_5^{(2)}$ and $\Omega_6^{(2)}$ indicate the stick domains, which are symbolized by pink and green, respectively; the velocity boundary is demonstrated by the $\partial\Omega_{12}^{(2)}$, which is shown by the black dashed line; the black dotted-dashed line, which can be seen as the boundary $\partial\Omega_{56}^{(2)}$, denotes the velocity boundary; the pink dashed lines at the boundaries $\partial\Omega_{15}^{(2)}$ and $\partial\Omega_{26}^{(2)}$ denote the stick boundaries.

4.2. Vector equations

Based on the boundaries and domains specified by using absolute coordinates, it is easy to transform the mass m_i's ($i \in \{1, 2\}$) motion equation into the vector form given by

$$\begin{aligned} &\dot{\mathbf{x}}_i^{(\delta_i)} = \mathbf{F}_i^{(\delta_i)}(\mathbf{x}_i^{(\delta_i)}, t), \ i \in \{1, 2\}, \\ &\delta_1 \in \{0, 1, 2, 3, 4\}, \ \delta_2 \in \{0, 1, 2\} \end{aligned} \tag{4.9}$$

for the mass m_1's non-left stick motion (i.e., it is also the mass m_2's non-stick motion), and

$$\begin{aligned} &\dot{\mathbf{x}}_i^{(\delta_i)} = \mathbf{H}_i^{(\delta_i)}(\mathbf{x}_i^{(\delta_i)}, \mathbf{x}_{\bar{i}}^{(\delta_{\bar{i}})}, t), \ \ i \neq \bar{i} \in \{1, 2\}, \\ &\delta_1 \in \{0, 5, 6, 7, 8\}, \ \ \delta_2 \in \{0, 5, 6\} \end{aligned} \tag{4.10}$$

for the mass m_1's left stick motion (i.e., it is also the mass m_2's stick motion), where

$$\begin{aligned} &\mathbf{x}_i^{(\delta_i)} \triangleq (x_i^{(\delta_i)}, \dot{x}_i^{(\delta_i)})^{\mathrm{T}}, \\ &\mathbf{F}_i^{(\delta_i)} \triangleq \mathbf{F}_i^{(\delta_i)}(\mathbf{x}_i^{(\delta_i)}, t) \equiv (\dot{x}_i^{(\delta_i)}, F_i^{(\delta_i)})^{\mathrm{T}}, \\ &\mathbf{H}_i^{(\delta_i)} \triangleq \mathbf{H}_i^{(\delta_i)}(\mathbf{x}_i^{(\delta_i)}, \mathbf{x}_{\bar{i}}^{(\delta_{\bar{i}})}, t) \equiv (\dot{x}_i^{(\delta_i)}, H_i^{(\delta_i)})^{\mathrm{T}}, \\ &F_i^{(\delta_i)} \triangleq F_i^{(\delta_i)}(\mathbf{x}_i^{(\delta_i)}, t), \ H_i^{(\delta_i)} \triangleq H_i^{(\delta_i)}(\mathbf{x}_i^{(\delta_i)}, \mathbf{x}_{\bar{i}}^{(\delta_{\bar{i}})}, t). \end{aligned} \tag{4.11}$$

Here, $\delta_1 = 0$ represents the following motions of the oscillator at the velocity boundaries: the sliding motion at the boundary $\partial\Omega_{12}^{(1)}$, the right stick-sliding motion at the boundary $\partial\Omega_{34}^{(1)}$, the left stick-sliding motion at the boundary $\partial\Omega_{56}^{(1)}$ and the double stick-sliding motion at the boundary $\partial\Omega_{78}^{(1)}$ for the mass m_1; $\delta_2 = 0$ indicates the following motions of the oscillator at the velocity boundaries: the sliding motion at the boundary $\partial\Omega_{12}^{(2)}$, and the stick-sliding motion at the boundary $\partial\Omega_{56}^{(2)}$ for the mass m_2. In this instance, the force on the mass m_i ($i \in \{1, 2\}$) per unit of mass is

$$F_i^{(0)} = 0 \text{ or } H_i^{(0)} = 0. \tag{4.12}$$

Free movement of object m_i ($i \in \{1, 2\}$) in domains $\Omega_1^{(i)}$ and $\Omega_2^{(i)}$ is indicated by $\delta_i = 1, 2$ ($i \in \{1, 2\}$), respectively; in domain $\Omega_3^{(1)}$ and $\Omega_4^{(1)}$, the object m_1 executes the right stick motion, as indicated by $\delta_1 = 3, 4$. The forces exerted on the masses m_i ($i = 1, 2$) per unit of mass are

$$\begin{cases} F_1^{(\delta_1)} = q_1 \sin(\Omega t + \varphi_1) + b_1 - k_1^{(1)} x_1 - k_2^{(1)} (x_1)^3 \\ \qquad - c_1^{(1)} \dot{x}_1 - c_2^{(1)} (\dot{x}_1)^3 - f^{(1)}, (\delta_1 = 1, 2); \\ F_1^{(\delta_1)} = q_1 \sin(\Omega t + \varphi_1) + b_1 - k_1^{(1)} x_1 - k_2^{(1)} (x_1)^3 \\ \qquad - c_1^{(1)} \dot{x}_1 - c_2^{(1)} (\dot{x}_1)^3 \\ \qquad - k_6^{(1)} (x_1 - d_1) - f^{(1)}, (\delta_1 = 3, 4); \\ F_2^{(\delta_2)} = q_2 \sin(\Omega t + \varphi_2) + b_2 - k_4^{(2)} x_2 - k_5^{(2)} (x_2)^3 \\ \qquad - c_4^{(2)} \dot{x}_2 - c_5^{(2)} (\dot{x}_2)^3 - f^{(2)}, (\delta_2 = 1, 2). \end{cases} \tag{4.13}$$

$\delta_i = 5, 6$ ($i \in \{1, 2\}$) expresses that, in domains $\Omega_5^{(i)}$ and $\Omega_6^{(i)}$, the object m_1 performs the left stick motion and the object m_2 performs the stick motion, respectively; in domains $\Omega_7^{(1)}$ and $\Omega_8^{(1)}$, the object m_1 performs the double stick motion, as indicated by $\delta_1 = 7, 8$. The forces exerted on the masses m_i ($i = 1, 2$) per unit of mass are

$$\begin{cases} H_1^{(\delta_1)} = q_1 \sin(\Omega t + \varphi_1) + b_1 - k_1^{(1)} x_1 - k_2^{(1)} (x_1)^3 \\ \qquad - c_1^{(1)} \dot{x}_1 - c_2^{(1)} (\dot{x}_1)^3 - k_3^{(1)} (x_1 - x_2 + d) \\ \qquad - c_3^{(1)} (\dot{x}_1 - \dot{x}_2) - f^{(1)}, \qquad (\delta_1 = 5, 6); \\ H_1^{(\delta_1)} = q_1 \sin(\Omega t + \varphi_1) + b_1 - k_1^{(1)} x_1 - k_2^{(1)} (x_1)^3 \\ \qquad - c_1^{(1)} \dot{x}_1 - c_2^{(1)} (\dot{x}_1)^3 - k_6^{(1)} (x_1 - d_1) \\ \qquad - c_3^{(1)} (\dot{x}_1 - \dot{x}_2) - k_3^{(1)} (x_1 - x_2 + d) \\ \qquad - f^{(1)}, \qquad (\delta_1 = 7, 8); \\ H_2^{(\delta_2)} = q_2 \sin(\Omega t + \varphi_2) + b_2 - k_4^{(2)} x_2 - k_5^{(2)} (x_2)^3 \\ \qquad - c_4^{(2)} \dot{x}_2 - c_5^{(2)} (\dot{x}_2)^3 - k_3^{(2)} (x_2 - x_1 - d) \\ \qquad - c_3^{(2)} (\dot{x}_2 - \dot{x}_1) - f^{(2)}, \qquad (\delta_2 = 5, 6). \end{cases} \tag{4.14}$$

Since the displacement boundary is tied to time in absolute coordinates, relative coordinates must be introduced to fully examine the two masses' switching rules at the displacement boundary. The following is a list of the relative variables:

$$\dot{z}_i = \dot{x}_i - \dot{x}_{\bar{i}},\ \ddot{z}_i = \ddot{x}_i - \ddot{x}_{\bar{i}},\ z_i = x_i - x_{\bar{i}},\ i \neq \bar{i} \in \{1, 2\}. \tag{4.15}$$

Because the object m_1's left stick motion appears and vanishes along with the object m_2's stick motion, it is possible to determine the situation of the object m_2's stick motion by studying the object m_1's left stick motion, where the domains for the mass m_1 are defined as follows in relative coordinates:

$$\left\{\begin{aligned}
\Omega_1^{(1)} &= \{(z_1, \dot{z}_1) \mid z_1 + x_2 < d_1,\ z_1 > -d,\ \dot{z}_1 > -\dot{x}_2\},\\
\Omega_2^{(1)} &= \{(z_1, \dot{z}_1) \mid z_1 + x_2 < d_1,\ z_1 > -d,\ \dot{z}_1 < -\dot{x}_2\},\\
\Omega_3^{(1)} &= \{(z_1, \dot{z}_1) \mid z_1 + x_2 > d_1,\ z_1 > -d,\ \dot{z}_1 > -\dot{x}_2\},\\
\Omega_4^{(1)} &= \{(z_1, \dot{z}_1) \mid z_1 + x_2 > d_1,\ z_1 > -d,\ \dot{z}_1 < -\dot{x}_2\},\\
\Omega_5^{(1)} &= \{(z_1, \dot{z}_1) \mid z_1 + x_2 < d_1,\ z_1 < -d,\ \dot{z}_1 > -\dot{x}_2\},\\
\Omega_6^{(1)} &= \{(z_1, \dot{z}_1) \mid z_1 + x_2 < d_1,\ z_1 < -d,\ \dot{z}_1 < -\dot{x}_2\},\\
\Omega_7^{(1)} &= \{(z_1, \dot{z}_1) \mid z_1 + x_2 > d_1,\ z_1 < -d,\ \dot{z}_1 > -\dot{x}_2\},\\
\Omega_8^{(1)} &= \{(z_1, \dot{z}_1) \mid z_1 + x_2 > d_1,\ z_1 < -d,\ \dot{z}_1 < -\dot{x}_2\},
\end{aligned}\right. \tag{4.16}$$

and the associated velocity boundaries and displacement boundaries are characterized as

$$\left\{\begin{aligned}
\partial\Omega_{34}^{(1)} = \partial\Omega_{43}^{(1)} &= \{(z_1, \dot{z}_1) \mid \varphi_{34}^{(1)} = \varphi_{43}^{(1)} \equiv \dot{z}_1 + \dot{x}_2 = 0,\\
&\qquad z_1 > -d,\ z_1 + x_2 > d_1\},\\
\partial\Omega_{56}^{(1)} = \partial\Omega_{65}^{(1)} &= \{(z_1, \dot{z}_1) \mid \varphi_{56}^{(1)} = \varphi_{65}^{(1)} \equiv \dot{z}_1 + \dot{x}_2 = 0,\\
&\qquad z_1 < -d,\ z_1 + x_2 < d_1\},\\
\partial\Omega_{78}^{(1)} = \partial\Omega_{87}^{(1)} &= \{(z_1, \dot{z}_1) \mid \varphi_{78}^{(1)} = \varphi_{87}^{(1)} \equiv \dot{z}_1 + \dot{x}_2 = 0,\\
&\qquad z_1 < -d,\ z_1 + x_2 > d_1\},\\
\partial\Omega_{15}^{(1)} = \partial\Omega_{51}^{(1)} &= \{(z_1, \dot{z}_1) \mid \varphi_{15}^{(1)} = \varphi_{51}^{(1)} \equiv z_1 + d = 0,\\
&\qquad \dot{z}_1 > -\dot{x}_2,\ z_1 + x_2 < d_1\},\\
\partial\Omega_{26}^{(1)} = \partial\Omega_{62}^{(1)} &= \{(z_1, \dot{z}_1) \mid \varphi_{26}^{(1)} = \varphi_{62}^{(1)} \equiv z_1 + d = 0,\\
&\qquad \dot{z}_1 < -\dot{x}_2,\ z_1 + x_2 < d_1\},\\
\partial\Omega_{37}^{(1)} = \partial\Omega_{73}^{(1)} &= \{(z_1, \dot{z}_1) \mid \varphi_{37}^{(1)} = \varphi_{73}^{(1)} \equiv z_1 + d = 0,\\
&\qquad \dot{z}_1 > -\dot{x}_2,\ z_1 + x_2 > d_1\},\\
\partial\Omega_{48}^{(1)} = \partial\Omega_{84}^{(1)} &= \{(z_1, \dot{z}_1) \mid \varphi_{48}^{(1)} = \varphi_{84}^{(1)} \equiv z_1 + d = 0,\\
&\qquad \dot{z}_1 < -\dot{x}_2,\ z_1 + x_2 > d_1\},\\
\partial\Omega_{13}^{(1)} = \partial\Omega_{31}^{(1)} &= \{(z_1, \dot{z}_1) \mid \varphi_{13}^{(1)} = \varphi_{31}^{(1)} \equiv z_1 + x_2 - d_1 = 0,\\
&\qquad \dot{z}_1 > -\dot{x}_2,\ z_1 > -d\},\\
\partial\Omega_{24}^{(1)} = \partial\Omega_{42}^{(1)} &= \{(z_1, \dot{z}_1) \mid \varphi_{24}^{(1)} = \varphi_{42}^{(1)} \equiv z_1 + x_2 - d_1 = 0,\\
&\qquad \dot{z}_1 < -\dot{x}_2,\ z_1 > -d\}.\\
\partial\Omega_{57}^{(1)} = \partial\Omega_{75}^{(1)} &= \{(z_1, \dot{z}_1) \mid \varphi_{57}^{(1)} = \varphi_{75}^{(1)} \equiv z_1 + x_2 - d_1 = 0,\\
&\qquad \dot{z}_1 > -\dot{x}_2,\ z_1 < -d\},\\
\partial\Omega_{68}^{(1)} = \partial\Omega_{86}^{(1)} &= \{(z_1, \dot{z}_1) \mid \varphi_{68}^{(1)} = \varphi_{86}^{(1)} \equiv z_1 + x_2 - d_1 = 0,\\
&\qquad \dot{z}_1 < -\dot{x}_2,\ z_1 < -d\}.
\end{aligned}\right. \tag{4.17}$$

The division of the mass m_1's domains and boundaries in relative coordinates are illustrated in Figure 5. The displacement boundaries $\partial\Omega_{15}^{(1)}$, $\partial\Omega_{37}^{(1)}$, $\partial\Omega_{48}^{(1)}$and $\partial\Omega_{26}^{(1)}$ become straight lines, which is conducive to analyzing the stick motion's switching conditions.

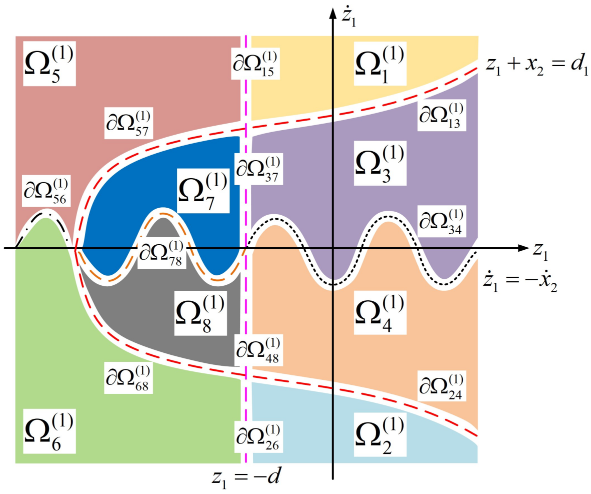

Figure 5. Domain and boundary partition of the mass m_1 in relative coordinates.

The object m_1's motion equation can be represented in vector form by using the relative coordinates for regions and boundaries, i.e.,

$$\dot{\mathbf{z}}_1^{(\delta_1)} = \mathbf{K}_1^{(\delta_1)}(\mathbf{z}_1^{(\delta_1)}, t),\ \ \delta_1 \in \{0, 1, 2, 3, 4\}, \tag{4.18}$$

for the mass m_1's non-left stick motion (i.e., it is also the mass m_2's non-stick motion), and

$$\dot{\mathbf{z}}_1^{(\delta_1)} = \mathbf{S}_1^{(\delta_1)}(\mathbf{z}_1^{(\delta_1)}, \mathbf{x}_2^{(\delta_2)}, t),\ \ \delta_1 \in \{0, 5, 6, 7, 8\},\ \ \delta_2 \in \{0, 5, 6\} \tag{4.19}$$

for the mass m_1's left stick motion (i.e., it is also the mass m_2's stick motion), where

$$\left.\begin{aligned}
&\mathbf{z}_1^{(\delta_1)} \triangleq (z_1^{(\delta_1)}, \dot{z}_1^{(\delta_1)})^{\mathrm{T}},\\
&\mathbf{K}_1^{(\delta_1)} \triangleq \mathbf{K}_1^{(\delta_1)}(\mathbf{z}_1^{(\delta_1)}, t) \equiv (\dot{z}_1^{(\delta_1)}, K_1^{(\delta_1)})^{\mathrm{T}},\\
&\mathbf{S}_1^{(\delta_1)} \triangleq \mathbf{S}_1^{(\delta_1)}(\mathbf{z}_1^{(\delta_1)}, \mathbf{x}_2^{(\delta_2)}, t) \equiv (\dot{z}_1^{(\delta_1)}, S_1^{(\delta_1)})^{\mathrm{T}},\\
&K_1^{(\delta_1)} \triangleq K_1^{(\delta_1)}(\mathbf{z}_1^{(\delta_1)}, t),\ S_1^{(\delta_1)} \triangleq S_1^{(\delta_1)}(\mathbf{z}_1^{(\delta_1)}, \mathbf{x}_2^{(\delta_2)}, t).
\end{aligned}\right\} \tag{4.20}$$

Similar to the absolute coordinates, δ_i ($i \in \{1, 2\}$) has the same meaning. It is simple to obtain the motion equations of (4.18)–(4.20) in the relative coordinates, in accordance with the equations of motion in absolute coordinates.

Because the discontinuous dynamical system presented in this paper has unequal static and dynamic friction forces, the velocity boundaries represented by $\partial\Omega_{\alpha\beta}^{(i)}$ ($i = 1, (\alpha,\beta) \in \{(1,2),(3,4),(5,6),(7,8)\}$, and $i = 2, (\alpha,\beta) \in \{(1,2),(5,6)\}$) have flow barriers. The flow barrier vector fields for $\mathbf{x}_m^{(i)} = (x_m^{(i)}, \dot{x}_m^{(i)}) \in \partial\Omega_{\alpha\beta}^{(i)}$ ($i = 1, (\alpha,\beta) \in \{(1,2),(3,4),(5,6),(7,8)\}$, and $i = 2, (\alpha,\beta) \in \{(1,2),(5,6)\}$) at time t_m are given as

$$\begin{aligned} &\mathbf{F}_i^{(0>0_\delta)}(\mathbf{x}_m^{(i)}, t_m, \tau^{(\delta)}) = (\dot{x}_m^{(i)}, F_i^{(0>0_\delta)}(\mathbf{x}_m^{(i)}, t_m, \tau^{(\delta)}))^{\mathrm{T}}, \\ &\quad i \in \{1,2\};\ \delta \in \{1,2,3,4\} \text{ if } i = 1, \\ &\quad \delta \in \{1,2\} \text{ if } i = 2;\ \text{ and } \tau^{(\delta)} \in [\tau_1^{(\delta)}, \tau_2^{(\delta)}], \end{aligned} \tag{4.21}$$

where

$$\begin{aligned} &F_1^{(0>0_\delta)}(\mathbf{x}_m^{(1)}, t_m, \tau^{(\delta)}) \\ &= q_1 \sin(\Omega t_m + \varphi_1) + b_1 - k_1^{(1)} x_m^{(1)} - k_2^{(1)} (x_m^{(1)})^3 \\ &\quad -c_1^{(1)} \dot{x}_m^{(1)} - c_2^{(1)} (\dot{x}_m^{(1)})^3 - f_{s1}^{(\delta)}(\tau^{(\delta)}), \quad (\delta = 1,2); \\ &F_1^{(0>0_\delta)}(\mathbf{x}_m^{(1)}, t_m, \tau^{(\delta)}) \\ &= q_1 \sin(\Omega t_m + \varphi_1) + b_1 - k_1^{(1)} x_m^{(1)} - k_2^{(1)} (x_m^{(1)})^3 \\ &\quad -c_1^{(1)} \dot{x}_m^{(1)} - c_2^{(1)} (\dot{x}_m^{(1)})^3 \\ &\quad -k_6^{(1)} (x_m^{(1)} - d_1) - f_{s1}^{(\delta)}(\tau^{(\delta)}), \qquad (\delta = 3,4); \\ &F_2^{(0>0_\delta)}(\mathbf{x}_m^{(2)}, t_m, \tau^{(\delta)}) \\ &= q_2 \sin(\Omega t_m + \varphi_2) + b_2 - k_4^{(2)} x_m^{(2)} - k_5^{(2)} (x_m^{(2)})^3 \\ &\quad -c_4^{(2)} \dot{x}_m^{(2)} - c_5^{(2)} (\dot{x}_m^{(2)})^3 - f_{s2}^{(\delta)}(\tau^{(\delta)}), \quad (\delta = 1,2) \end{aligned} \tag{4.22}$$

for the mass m_1's non-left stick motion (i.e., it is also the mass m_2's non-stick motion), and

$$\begin{aligned} &\mathbf{H}_i^{(0>0_\delta)}(\mathbf{x}_m^{(i)}, t_m, \tau^{(\delta)}) = \mathbf{H}_i^{(0>0_\delta)}(\mathbf{x}_m^{(i)}, \mathbf{x}_{\bar{i}}^{(\delta_{\bar{i}})}, t_m, \tau^{(\delta)}) \\ &= (\dot{x}_m^{(i)}, H_i^{(0>0_\delta)}(\mathbf{x}_m^{(i)}, \mathbf{x}_{\bar{i}}^{(\delta_{\bar{i}})}, t_m, \tau^{(\delta)}))^{\mathrm{T}}, \\ &\quad i \neq \bar{i} \in \{1,2\};\ \tau^{(\delta)} \in [\tau_1^{(\delta)}, \tau_2^{(\delta)}]; \\ &\quad \delta \in \{5,6,7,8\} \text{ if } i = 1, \\ &\quad \delta \in \{5,6\} \text{ if } i = 2; \\ &\quad \text{and } \delta_1 \in \{0,5,6,7,8\}, \delta_2 \in \{0,5,6\}, \end{aligned} \tag{4.23}$$

where

$$\begin{aligned} &H_1^{(0>0_\delta)}(\mathbf{x}_m^{(1)}, \mathbf{x}_2^{(\delta_2)}, t_m, \tau^{(\delta)}) \\ &= q_1 \sin(\Omega t_m + \varphi_1) + b_1 - k_1^{(1)} x_m^{(1)} - k_2^{(1)} (x_m^{(1)})^3 \\ &\quad -c_1^{(1)} \dot{x}_m^{(1)} - c_2^{(1)} (\dot{x}_m^{(1)})^3 - k_3^{(1)} (x_m^{(1)} - x_m^{(2)} + d) \\ &\quad -c_3^{(1)} (\dot{x}_m^{(1)} - \dot{x}_m^{(2)}) - f_{s1}^{(\delta)}(\tau^{(\delta)}), \qquad (\delta = 5,6); \\ &H_1^{(0>0_\delta)}(\mathbf{x}_m^{(1)}, \mathbf{x}_2^{(\delta_2)}, t_m, \tau^{(\delta)}) \\ &= q_1 \sin(\Omega t_m + \varphi_1) + b_1 - k_1^{(1)} x_m^{(1)} - k_2^{(1)} (x_m^{(1)})^3 \\ &\quad -c_1^{(1)} \dot{x}_m^{(1)} - c_2^{(1)} (\dot{x}_m^{(1)})^3 - k_6^{(1)} (x_m^{(1)} - d_1) \\ &\quad -c_3^{(1)} (\dot{x}_m^{(1)} - \dot{x}_m^{(2)}) - k_3^{(1)} (x_m^{(1)} - x_m^{(2)} + d) \\ &\quad -f_{s1}^{(\delta)}(\tau^{(\delta)}), \qquad (\delta = 7,8); \\ &H_2^{(0>0_\delta)}(\mathbf{x}_m^{(2)}, \mathbf{x}_1^{(\delta_1)}, t_m, \tau^{(\delta)}) \\ &= q_2 \sin(\Omega t_m + \varphi_2) + b_2 - k_4^{(2)} x_m^{(2)} - k_5^{(2)} (x_m^{(2)})^3 \\ &\quad -c_4^{(2)} \dot{x}_m^{(2)} - c_5^{(2)} (\dot{x}_m^{(2)})^3 - k_3^{(2)} (x_m^{(2)} - x_m^{(1)} - d) \\ &\quad -c_3^{(2)} (\dot{x}_m^{(2)} - \dot{x}_m^{(1)}) - f_{s2}^{(\delta)}(\tau^{(\delta)}), \qquad (\delta = 5,6) \end{aligned} \tag{4.24}$$

for the mass m_1's left stick motion (i.e., it is also the mass m_2's stick motion), and

$$\begin{aligned} &f_{s1}^{(\alpha)}(\tau^{(\alpha)}) \in (-\infty, \mu_s g] \text{ and } f_{s1}^{(\beta)}(\tau^{(\beta)}) \in [-\mu_s g, +\infty) \\ &\quad \text{for } (\alpha,\beta) \in \{(1,2),(3,4),(5,6),(7,8)\}, \\ &f_{s2}^{(\alpha)}(\tau^{(\alpha)}) \in [-\mu_s g, +\infty) \text{ and } f_{s2}^{(\beta)}(\tau^{(\beta)}) \in (-\infty, \mu_s g] \\ &\quad \text{for } (\alpha,\beta) \in \{(1,2),(5,6)\}. \end{aligned} \tag{4.25}$$

The δ-side ($\delta \in \{1,2,3,4,5,6,7,8\}$) boundary flow barriers for $\mathbf{x}_m^{(i)} = (x_m^{(i)}, \dot{x}_m^{(i)}) \in \partial\Omega_{\alpha\beta}^{(i)}$, $i = 1, (\alpha,\beta) \in \{(1,2),(3,4),(5,6),(7,8)\}$; and $i = 2, (\alpha,\beta) \in \{(1,2),(5,6)\}$) at time t_m are given below.

If $\tau^{(\delta)} = \tau_1^{(\delta)}$, the expression for the flow barrier can be obtained by replacing $\tau^{(\delta)}$ in Eq (4.22) or Eq (4.24) with $\tau_1^{(\delta)}$; and if $\tau^{(\delta)} = \tau_2^{(\delta)}$, the expression for the flow barrier can be obtained by applying

$$\begin{aligned} &\mathbf{F}_1^{(0>0_1)}(\mathbf{x}_m^{(1)}, t_m, \tau_2^{(1)}) = (\dot{x}_m^{(1)}, +\infty)^{\mathrm{T}}, \\ &\mathbf{F}_1^{(0>0_2)}(\mathbf{x}_m^{(1)}, t_m, \tau_2^{(2)}) = (\dot{x}_m^{(1)}, -\infty)^{\mathrm{T}}, \\ &\mathbf{F}_1^{(0>0_3)}(\mathbf{x}_m^{(1)}, t_m, \tau_2^{(3)}) = (\dot{x}_m^{(1)}, +\infty)^{\mathrm{T}}, \\ &\mathbf{F}_1^{(0>0_4)}(\mathbf{x}_m^{(1)}, t_m, \tau_2^{(4)}) = (\dot{x}_m^{(1)}, -\infty)^{\mathrm{T}}, \\ &\mathbf{F}_2^{(0>0_1)}(\mathbf{x}_m^{(2)}, t_m, \tau_2^{(1)}) = (\dot{x}_m^{(2)}, -\infty)^{\mathrm{T}}, \\ &\mathbf{F}_2^{(0>0_2)}(\mathbf{x}_m^{(2)}, t_m, \tau_2^{(2)}) = (\dot{x}_m^{(2)}, +\infty)^{\mathrm{T}} \end{aligned} \tag{4.26}$$

for the mass m_1's non-left stick motion (i.e., it is also the mass m_2's non-stick motion), and

$$\begin{aligned} &\mathbf{H}_1^{(0>0_5)}(\mathbf{x}_m^{(1)}, t_m, \tau_2^{(5)}) = (\dot{x}_m^{(1)}, +\infty)^{\mathrm{T}}, \\ &\mathbf{F}_1^{(0>0_6)}(\mathbf{x}_m^{(1)}, t_m, \tau_2^{(6)}) = (\dot{x}_m^{(1)}, -\infty)^{\mathrm{T}}, \\ &\mathbf{H}_1^{(0>0_7)}(\mathbf{x}_m^{(1)}, t_m, \tau_2^{(7)}) = (\dot{x}_m^{(1)}, +\infty)^{\mathrm{T}}, \\ &\mathbf{F}_1^{(0>0_8)}(\mathbf{x}_m^{(1)}, t_m, \tau_2^{(8)}) = (\dot{x}_m^{(1)}, -\infty)^{\mathrm{T}}, \\ &\mathbf{H}_2^{(0>0_5)}(\mathbf{x}_m^{(2)}, t_m, \tau_2^{(5)}) = (\dot{x}_m^{(2)}, -\infty)^{\mathrm{T}}, \\ &\mathbf{F}_2^{(0>0_6)}(\mathbf{x}_m^{(2)}, t_m, \tau_2^{(6)}) = (\dot{x}_m^{(2)}, +\infty)^{\mathrm{T}} \end{aligned} \tag{4.27}$$

for the mass m_1's left stick motion (i.e., it is also the mass m_2's stick motion).

5. Analytical conditions

This section will discuss the flow switchability conditions on discontinuous/nonsmooth boundaries for this 2-DOF frictional vibration system. At the separation boundaries, the normal vectors and the G-functions are first given; then, the switching criteria of flow are provided.

In absolute coordinates, the normal vectors of the displacement boundaries $\partial\Omega_{ln}^{(1)}$ ($(l,n) \in \{(1,3),(2,4),(5,7),(6,8)\}$) and the velocity boundaries $\partial\Omega_{\alpha\beta}^{(i)}$ ($(\alpha,\beta) \in \{(1,2),$

$(3,4),(5,6),(7,8)\}$ if $i=1$; and $(\alpha,\beta)\in\{(1,2),(5,6)\}$ if $i=2$) are respectively provided as

$$\mathbf{n}_{\partial\Omega_{ln}^{(1)}} \equiv {}^{t}\mathbf{n}_{\partial\Omega_{ln}^{(1)}} = \nabla\varphi_{ln}^{(1)} = (\frac{\partial\varphi_{ln}^{(1)}}{\partial x_1}, \frac{\partial\varphi_{ln}^{(1)}}{\partial \dot{x}_1})^{\mathrm{T}} = (1,0)^{\mathrm{T}}, \quad (5.1)$$

$$\mathbf{n}_{\partial\Omega_{\alpha\beta}^{(i)}} \equiv {}^{t}\mathbf{n}_{\partial\Omega_{\alpha\beta}^{(i)}} = \nabla\varphi_{\alpha\beta}^{(i)} = (\frac{\partial\varphi_{\alpha\beta}^{(i)}}{\partial x_i}, \frac{\partial\varphi_{\alpha\beta}^{(i)}}{\partial \dot{x}_i})^{\mathrm{T}} = (0,1)^{\mathrm{T}}, \quad (5.2)$$

where $\nabla = (\frac{\partial}{\partial x}, \frac{\partial}{\partial \dot{x}})^{\mathrm{T}}$.

In relative coordinates, the normal vectors of the displacement boundaries $\partial\Omega_{ln}^{(1)}$ $((l,n)\in\{(1,5),(2,6),(3,7),(4,8)\})$ are denoted by

$$\mathbf{n}_{\partial\Omega_{ln}^{(1)}} \equiv {}^{t}\mathbf{n}_{\partial\Omega_{ln}^{(1)}} = \nabla\varphi_{ln}^{(1)} = (\frac{\partial\varphi_{ln}^{(1)}}{\partial z_1}, \frac{\partial\varphi_{ln}^{(1)}}{\partial \dot{z}_1})^{\mathrm{T}} = (1,0)^{\mathrm{T}}, \quad (5.3)$$

where $\nabla = (\frac{\partial}{\partial x}, \frac{\partial}{\partial \dot{x}})^{\mathrm{T}}$.

We assume, for simplicity, that the mass m_i's ($i\in\{1,2\}$) motion flow arrives at the separation boundary point $\mathbf{x}_m^{(i)}$ at time t_m, and $t_{m\pm}=t_m\pm 0$.

Definition 5.1. *At the velocity boundary $\partial\Omega_{\alpha\beta}^{(i)}$ ($\alpha\neq\beta\in\{1,2\}$ or $\{3,4\}$ or $\{5,6\}$ or $\{7,8\}$ if $i=1$; $\alpha\neq\beta\in\{1,2\}$ or $\{5,6\}$ if $i=2$), the following is a list of the 0th-order and first-order G-functions at time t_m in absolute coordinates:*

$$\begin{aligned}
G_{\partial\Omega_{\alpha\beta}^{(i)}}^{(0,\delta)}(t_{m\pm}) &\equiv \mathrm{G}_{\partial\Omega_{\alpha\beta}^{(i)}}^{(0,\delta)}(\mathbf{x}_m^{(i)},t_{m\pm}) \\
&= \mathbf{n}_{\partial\Omega_{\alpha\beta}^{(i)}}^{\mathrm{T}}\cdot\mathbf{F}_i^{(\delta)}(\mathbf{x}_m^{(i)},t_{m\pm}) \\
&= F_i^{(\delta)}(\mathbf{x}_m^{(i)},t_{m\pm}), \\
G_{\partial\Omega_{\alpha\beta}^{(i)}}^{(1,\delta)}(t_{m\pm}) &\equiv \mathrm{G}_{\partial\Omega_{\alpha\beta}^{(i)}}^{(1,\delta)}(\mathbf{x}_m^{(i)},t_{m\pm}) \\
&= \mathbf{n}_{\partial\Omega_{\alpha\beta}^{(i)}}^{\mathrm{T}}\cdot D\mathbf{F}_i^{(\delta)}(\mathbf{x}_m^{(i)},t_{m\pm}) \\
&= DF_i^{(\delta)}(\mathbf{x}_m^{(i)},t_{m\pm}),
\end{aligned} \quad (5.4)$$

where $\alpha\neq\beta\in\{1,2\}$ or $\{3,4\}$ if $i=1$; $\alpha\neq\beta\in\{1,2\}$ if $i=2,\delta\in\{\alpha,\beta\}$; and,

$$\begin{aligned}
G_{\partial\Omega_{\alpha\beta}^{(i)}}^{(0,\delta)}(t_{m\pm}) &\equiv \mathrm{G}_{\partial\Omega_{\alpha\beta}^{(i)}}^{(0,\delta)}(\mathbf{x}_m^{(i)},t_{m\pm}) \\
&= \mathbf{n}_{\partial\Omega_{\alpha\beta}^{(i)}}^{\mathrm{T}}\cdot\mathbf{H}_i^{(\delta)}(\mathbf{x}_m^{(i)},t_{m\pm}) \\
&= H_i^{(\delta)}(\mathbf{x}_m^{(i)},t_{m\pm}), \\
G_{\partial\Omega_{\alpha\beta}^{(i)}}^{(1,\delta)}(t_{m\pm}) &\equiv \mathrm{G}_{\partial\Omega_{\alpha\beta}^{(i)}}^{(1,\delta)}(\mathbf{x}_m^{(i)},t_{m\pm}) \\
&= \mathbf{n}_{\partial\Omega_{\alpha\beta}^{(i)}}^{\mathrm{T}}\cdot D\mathbf{H}_i^{(\delta)}(\mathbf{x}_m^{(i)},t_{m\pm}) \\
&= DH_i^{(\delta)}(\mathbf{x}_m^{(i)},t_{m\pm}),
\end{aligned} \quad (5.5)$$

where $\alpha\neq\beta\in\{5,6\}$ or $\{7,8\}$ if $i=1$; $\alpha\neq\beta\in\{5,6\}$ if $i=2,\delta\in\{\alpha,\beta\}$. Here, $\mathbf{x}_i^{(\delta)}(t_{m\pm})=\mathbf{x}_i^{(0)}(t_m)=\mathbf{x}_m^{(i)}\in\partial\Omega_{\alpha\beta}^{(i)}$ ($\alpha\neq\beta\in\{1,2\}$ or $\{3,4\}$ or $\{5,6\}$ or $\{7,8\}$ if $i=1$; $\alpha\neq\beta\in\{1,2\}$ or $\{5,6\}$ if $i=2$).

Definition 5.2. *In absolute coordinates, at the displacement boundary $\partial\Omega_{ln}^{(1)}$ ($l\neq n\in\{1,3\}$ or $\{2,4\}$ or $\{5,7\}$ or $\{6,8\}$), the following is a list of the 0th-order and first-order G-functions at time t_m:*

$$\begin{aligned}
G_{\partial\Omega_{ln}^{(1)}}^{(0,\delta)}(t_{m\pm}) &\equiv \mathrm{G}_{\partial\Omega_{ln}^{(1)}}^{(0,\delta)}(\mathbf{x}_m^{(1)},t_{m\pm}) \\
&= \mathbf{n}_{\partial\Omega_{ln}^{(1)}}^{\mathrm{T}}\cdot\mathbf{F}_1^{(\delta)}(\mathbf{x}_m^{(1)},t_{m\pm}) \\
&= \dot{x}_1^{(\delta)}(t_{m\pm}), \\
G_{\partial\Omega_{ln}^{(1)}}^{(1,\delta)}(t_{m\pm}) &\equiv \mathrm{G}_{\partial\Omega_{ln}^{(1)}}^{(1,\delta)}(\mathbf{x}_m^{(1)},t_{m\pm}) \\
&= \mathbf{n}_{\partial\Omega_{ln}^{(1)}}^{\mathrm{T}}\cdot D\mathbf{F}_1^{(\delta)}(\mathbf{x}_m^{(1)},t_{m\pm}) \\
&= F_1^{(\delta)}(\mathbf{x}_m^{(1)},t_{m\pm}),
\end{aligned} \quad (5.6)$$

where $l\neq n\in\{1,3\}$ or $\{2,4\},\delta\in\{l,n\}$; and,

$$\begin{aligned}
G_{\partial\Omega_{ln}^{(1)}}^{(0,\delta)}(t_{m\pm}) &\equiv \mathrm{G}_{\partial\Omega_{ln}^{(1)}}^{(0,\delta)}(\mathbf{x}_m^{(1)},t_{m\pm}) \\
&= \mathbf{n}_{\partial\Omega_{ln}^{(1)}}^{\mathrm{T}}\cdot\mathbf{H}_1^{(\delta)}(\mathbf{x}_m^{(1)},t_{m\pm}) = \dot{x}_1^{(\delta)}(t_{m\pm}), \\
G_{\partial\Omega_{ln}^{(1)}}^{(1,\delta)}(t_{m\pm}) &\equiv \mathrm{G}_{\partial\Omega_{ln}^{(1)}}^{(1,\delta)}(\mathbf{x}_m^{(1)},t_{m\pm}) \\
&= \mathbf{n}_{\partial\Omega_{ln}^{(1)}}^{\mathrm{T}}\cdot D\mathbf{H}_1^{(\delta)}(\mathbf{x}_m^{(1)},t_{m\pm}) = H_1^{(\delta)}(\mathbf{x}_m^{(1)},t_{m\pm}),
\end{aligned} \quad (5.7)$$

where $l\neq n\in\{5,7\}$ or $\{6,8\},\delta\in\{l,n\}$.

Here, $\mathbf{x}_1^{(\delta)}(t_{m\pm})=\mathbf{x}_1^{(0)}(t_m)=\mathbf{x}_m^{(1)}\in\partial\Omega_{ln}^{(1)}$ ($l\neq n\in\{1,3\}$ or $\{2,4\}$ or $\{5,7\}$ or $\{6,8\}$).

Definition 5.3. *At the velocity boundary with the flow barrier $\partial\Omega_{\alpha\beta}^{(i)}$ ($\alpha\neq\beta\in\{1,2\}$ or $\{3,4\}$ or $\{5,6\}$ or $\{7,8\}$ if $i=1$; $\alpha\neq\beta\in\{1,2\}$ or $\{5,6\}$ if $i=2$), the following is a list of the 0th-order and first-order G-functions at time t_m in absolute coordinates:*

$$\begin{aligned}
G_{\partial\Omega_{\alpha\beta}^{(i)}}^{(0,0>0_\delta)}(t_{m\pm}) &\equiv \mathrm{G}_{\partial\Omega_{\alpha\beta}^{(i)}}^{(0,0>0_\delta)}(\mathbf{x}_m^{(i)},t_{m\pm},\tau^{(\delta)}) \\
&= \mathbf{n}_{\partial\Omega_{\alpha\beta}^{(i)}}^{\mathrm{T}}\cdot\mathbf{F}_i^{(0>0_\delta)}(\mathbf{x}_m^{(i)},t_{m\pm},\tau^{(\delta)}) \\
&= F_i^{(0>0_\delta)}(\mathbf{x}_m^{(i)},t_{m\pm},\tau^{(\delta)}), \\
G_{\partial\Omega_{\alpha\beta}^{(i)}}^{(1,0>0_\delta)}(t_{m\pm}) &\equiv \mathrm{G}_{\partial\Omega_{\alpha\beta}^{(i)}}^{(1,0>0_\delta)}(\mathbf{x}_m^{(i)},t_{m\pm},\tau^{(\delta)}) \\
&= \mathbf{n}_{\partial\Omega_{\alpha\beta}^{(i)}}^{\mathrm{T}}\cdot D\mathbf{F}_i^{(0>0_\delta)}(\mathbf{x}_m^{(i)},t_{m\pm},\tau^{(\delta)}) \\
&= DF_i^{(0>0_\delta)}(\mathbf{x}_m^{(i)},t_{m\pm},\tau^{(\delta)})
\end{aligned} \quad (5.8)$$

for $\alpha\neq\beta\in\{1,2\}$ or $\{3,4\}$ if $i=1$; $\alpha\neq\beta\in\{1,2\}$ if $i=2,\delta\in\{\alpha,\beta\}$; and,

$$\begin{aligned}
G_{\partial\Omega_{\alpha\beta}^{(i)}}^{(0,0>0_\delta)}(t_{m\pm}) &\equiv \mathrm{G}_{\partial\Omega_{\alpha\beta}^{(i)}}^{(0,0>0_\delta)}(\mathbf{x}_m^{(i)},t_{m\pm},\tau^{(\delta)}) \\
&= \mathbf{n}_{\partial\Omega_{\alpha\beta}^{(i)}}^{\mathrm{T}}\cdot\mathbf{H}_i^{(0>0_\delta)}(\mathbf{x}_m^{(i)},t_{m\pm},\tau^{(\delta)}) \\
&= H_i^{(0>0_\delta)}(\mathbf{x}_m^{(i)},t_{m\pm},\tau^{(\delta)}), \\
G_{\partial\Omega_{\alpha\beta}^{(i)}}^{(1,0>0_\delta)}(t_{m\pm}) &\equiv \mathrm{G}_{\partial\Omega_{\alpha\beta}^{(i)}}^{(1,0>0_\delta)}(\mathbf{x}_m^{(i)},t_{m\pm},\tau^{(\delta)}) \\
&= \mathbf{n}_{\partial\Omega_{\alpha\beta}^{(i)}}^{\mathrm{T}}\cdot D\mathbf{H}_i^{(0>0_\delta)}(\mathbf{x}_m^{(i)},t_{m\pm},\tau^{(\delta)}) \\
&= DH_i^{(0>0_\delta)}(\mathbf{x}_m^{(i)},t_{m\pm},\tau^{(\delta)})
\end{aligned} \quad (5.9)$$

for $\alpha \neq \beta \in \{5,6\}$ *or* $\{7,8\}$ *if* $i = 1$; $\alpha \neq \beta \in \{5,6\}$ *if* $i = 2$, $\delta \in \{\alpha,\beta\}$.

Here, $\mathbf{x}_i^{(\delta)}(t_{m\pm}) = \mathbf{x}_i^{(0)}(t_m) = \mathbf{x}_m^{(i)} \in \partial\Omega_{\alpha\beta}^{(i)}$ ($\alpha \neq \beta \in \{1,2\}$ or $\{3,4\}$ or $\{5,6\}$ or $\{7,8\}$ if $i = 1$; $\alpha \neq \beta \in \{1,2\}$ or $\{5,6\}$ if $i = 2$).

Definition 5.4. *In relative coordinates, at the displacement boundary* $\partial\Omega_{ln}^{(1)}$ ($l \neq n \in \{1,5\}$ or $\{2,6\}$ or $\{3,7\}$ or $\{4,8\}$)*, the following is a list of the* 0*th-order and first-order* G*-functions at time* t_m*:*

$$\begin{aligned} G_{\partial\Omega_{ln}^{(1)}}^{(0,\delta)}(t_{m\pm}) &\equiv \mathrm{G}_{\partial\Omega_{ln}^{(1)}}^{(0,\delta)}(\mathbf{z}_m^{(1)}, t_{m\pm}) \\ &= \mathbf{n}_{\partial\Omega_{ln}^{(1)}}^{\mathrm{T}} \cdot \mathbf{K}_1^{(\delta)}(\mathbf{z}_m^{(1)}, t_{m\pm}) = \dot{z}_1^{(\delta)}(\mathbf{z}_m^{(i)}, t_{m\pm}), \\ G_{\partial\Omega_{ln}^{(1)}}^{(1,\delta)}(t_{m\pm}) &\equiv \mathrm{G}_{\partial\Omega_{ln}^{(1)}}^{(1,\delta)}(\mathbf{z}_m^{(1)}, t_{m\pm}) \\ &= \mathbf{n}_{\partial\Omega_{ln}^{(1)}}^{\mathrm{T}} \cdot D\mathbf{K}_1^{(\delta)}(\mathbf{z}_m^{(1)}, t_{m\pm}) = K_1^{(\delta)}(\mathbf{z}_m^{(1)}, t_{m\pm}) \end{aligned} \tag{5.10}$$

for $\delta \in \{1,2,3,4\}$*; and,*

$$\begin{aligned} G_{\partial\Omega_{ln}^{(1)}}^{(0,\delta)}(t_{m\pm}) &\equiv \mathrm{G}_{\partial\Omega_{ln}^{(1)}}^{(0,\delta)}(\mathbf{z}_m^{(1)}, t_{m\pm}) \\ &= \mathbf{n}_{\partial\Omega_{ln}^{(1)}}^{\mathrm{T}} \cdot \mathbf{S}_1^{(\delta)}(\mathbf{z}_m^{(1)}, t_{m\pm}) = \dot{z}_i^{(\delta)}(\mathbf{z}_m^{(1)}, t_{m\pm}), \\ G_{\partial\Omega_{ln}^{(1)}}^{(1,\delta)}(t_{m\pm}) &\equiv \mathrm{G}_{\partial\Omega_{ln}^{(1)}}^{(1,\delta)}(\mathbf{z}_m^{(1)}, t_{m\pm}) \\ &= \mathbf{n}_{\partial\Omega_{ln}^{(1)}}^{\mathrm{T}} \cdot D\mathbf{S}_1^{(\delta)}(\mathbf{z}_m^{(1)}, t_{m\pm}) = S_1^{(\delta)}(\mathbf{z}_m^{(1)}, t_{m\pm}) \end{aligned} \tag{5.11}$$

for $\delta \in \{5,6,7,8\}$.

Here, $\mathbf{z}_1^{(\delta)}(t_{m\pm}) = \mathbf{z}_1^{(0)}(t_m) = \mathbf{z}_m^{(1)} \in \partial\Omega_{ln}^{(1)}$ ($l \neq n \in \{1,5\}$ or $\{2,6\}$ or $\{3,7\}$ or $\{4,8\}$).

5.1. At velocity boundaries in absolute coordinates

After the above discussion, one is able to determine the analytical criteria of the sliding motion, grazing flow and passable motion at the velocity boundary $\partial\Omega_{\alpha\beta}^{(i)}$ ($\alpha \neq \beta \in \{1,2\}$ or $\{3,4\}$ or $\{5,6\}$ or $\{7,8\}$ if $i = 1$; $\alpha \neq \beta \in \{1,2\}$ or $\{5,6\}$ if $i = 2$) for this 2-DOF frictional vibration system.

Theorem 5.1. *The passable motion's flow from* $\Omega_\alpha^{(i)}$ *to* $\Omega_\beta^{(i)}$ *at* $\mathbf{x}_m^{(i)} \in \partial\Omega_{\alpha\beta}^{(i)}$ ($\alpha \neq \beta \in \{1,2\}$ or $\{3,4\}$ or $\{5,6\}$ or $\{7,8\}$ if $i = 1$; $\alpha \neq \beta \in \{1,2\}$ or $\{5,6\}$ if $i = 2$) *at time* t_m *occurs if and only if*

$$\begin{aligned} &(-1)^{i+\alpha} F_i^{(\alpha)}(\mathbf{x}_m^{(i)}, t_{m-}) < 0 \text{ and} \\ &(-1)^{i+\alpha} F_i^{(\beta)}(\mathbf{x}_m^{(i)}, t_{m+}) < 0 \\ &\quad \text{for } \Omega_\alpha^{(i)} \to \Omega_\beta^{(i)}, \\ &\quad \alpha \neq \beta \in \{1,2\} \text{ or } \{3,4\} \text{ if } i = 1; \\ &\quad \alpha \neq \beta \in \{1,2\} \text{ if } i = 2; \end{aligned} \tag{5.12}$$

$$\begin{aligned} &(-1)^{i+\alpha} H_i^{(\alpha)}(\mathbf{x}_m^{(i)}, t_{m-}) < 0 \text{ and} \\ &(-1)^{i+\alpha} H_i^{(\beta)}(\mathbf{x}_m^{(i)}, t_{m+}) < 0 \\ &\quad \text{for } \Omega_\alpha^{(i)} \to \Omega_\beta^{(i)}, \\ &\quad \alpha \neq \beta \in \{5,6\} \text{ or } \{7,8\} \text{ if } i = 1; \\ &\quad \alpha \neq \beta \in \{5,6\} \text{ if } i = 2. \end{aligned} \tag{5.13}$$

Proof. At the time t_m, the flow of motion that has reached the boundary. The mass m_i ($i \in \{1,2\}$) is in motion on the ground with a nonzero speed before or after t_m, and, at time t_m, the mass m_i's ($i \in \{1,2\}$) velocity is zero. At time t_m, based on Luo's theory of flow switchability [42], the passable motion to occur at $\mathbf{x}_m^{(i)} \in \partial\Omega_{12}^{(i)}$ ($i \in \{1,2\}$) satisfies the following criteria:

$$\left.\begin{aligned} &(-1)^i G_{\partial\Omega_{12}^{(i)}}^{(0,1)}(\mathbf{x}_m^{(i)}, t_{m-}) > 0, \\ &(-1)^i G_{\partial\Omega_{12}^{(i)}}^{(0,2)}(\mathbf{x}_m^{(i)}, t_{m+}) > 0 \end{aligned}\right\} \text{ for } \Omega_1^{(i)} \to \Omega_2^{(i)}. \tag{5.14}$$

With Eq (5.2) and Eq (5.4), one obtains

$$\left.\begin{aligned} G_{\partial\Omega_{12}^{(i)}}^{(0,1)}(\mathbf{x}_m^{(i)}, t_{m\pm}) &= \mathbf{n}_{\partial\Omega_{12}^{(i)}}^{\mathrm{T}} \cdot \mathbf{F}_i^{(1)}(\mathbf{x}_m^{(i)}, t_{m\pm}) = F_i^{(1)}(t_{m\pm}), \\ G_{\partial\Omega_{12}^{(i)}}^{(0,2)}(\mathbf{x}_m^{(i)}, t_{m\pm}) &= \mathbf{n}_{\partial\Omega_{12}^{(i)}}^{\mathrm{T}} \cdot \mathbf{F}_i^{(2)}(\mathbf{x}_m^{(i)}, t_{m\pm}) = F_i^{(2)}(t_{m\pm}). \end{aligned}\right\} \tag{5.15}$$

From Eqs (5.14) and (5.15), the passable-flow-appearing conditions in Eq (5.12) for $\alpha = 1$ and $\beta = 2$ are obtained. Similar methods can be used to generate the other criteria in Eqs (5.12) and (5.13). □

Theorem 5.2. *(i) The sliding motion at* $\mathbf{x}_m^{(i)} \in \partial\Omega_{12}^{(i)}$ ($i \in \{1,2\}$) *at time* t_m *exists if and only if*

$$(-1)^i F_i^{(1)}(\mathbf{x}_m^{(i)}, t_{m-}) > 0 \text{ and } (-1)^i F_i^{(2)}(\mathbf{x}_m^{(i)}, t_{m-}) < 0. \tag{5.16}$$

(ii) The mass m_1*'s right stick-sliding motion at* $\mathbf{x}_m^{(1)} \in \partial\Omega_{34}^{(1)}$ *at time* t_m *exists if and only if*

$$F_1^{(3)}(\mathbf{x}_m^{(1)}, t_{m-}) < 0 \text{ and } F_1^{(4)}(\mathbf{x}_m^{(1)}, t_{m-}) > 0. \tag{5.17}$$

(iii) The mass m_1*'s left stick-sliding motion or the mass* m_2*'s stick-sliding motion at* $\mathbf{x}_m^{(i)} \in \partial\Omega_{56}^{(i)}$ ($i \in \{1,2\}$) *at time* t_m *exists if and only if*

$$\begin{aligned} &(-1)^i H_i^{(5)}(\mathbf{x}_m^{(i)}, t_{m-}) > 0 \text{ and} \\ &(-1)^i H_i^{(6)}(\mathbf{x}_m^{(i)}, t_{m-}) < 0. \end{aligned} \tag{5.18}$$

(iv) The mass m_1*'s double stick-sliding motion at* $\mathbf{x}_m^{(1)} \in \partial\Omega_{78}^{(1)}$ *at time* t_m *exists if and only if*

$$H_1^{(7)}(\mathbf{x}_m^{(1)}, t_{m-}) < 0 \text{ and } H_1^{(8)}(\mathbf{x}_m^{(1)}, t_{m-}) > 0. \tag{5.19}$$

Proof. With relation to the ground, the object m_i ($i \in \{1,2\}$) is immobile; according to Luo's flow switchability theory [42], at the velocity boundary, a sink flow will be present. The mass m_1's left stick-sliding motion existing at $\mathbf{x}_m^{(1)} \in \partial\Omega_{56}^{(1)}$ or the mass m_2's stick-sliding motion existing at $\mathbf{x}_m^{(2)} \in \partial\Omega_{56}^{(2)}$ at time t_m satisfies the following conditions:

$$\left.\begin{aligned} &(-1)^i G^{(0,5)}_{\partial\Omega_{56}^{(i)}}(\mathbf{x}_m^{(i)}, t_{m-}) > 0 \text{ and} \\ &(-1)^i G^{(0,6)}_{\partial\Omega_{56}^{(i)}}(\mathbf{x}_m^{(i)}, t_{m-}) < 0, \ (i \in \{1,2\}). \end{aligned}\right. \tag{5.20}$$

With Eqs (5.2) and (5.5), one obtains

$$\left.\begin{aligned} G^{(0,5)}_{\partial\Omega_{56}^{(i)}}(\mathbf{x}_m^{(i)}, t_{m\pm}) = \mathbf{n}^{\mathrm{T}}_{\partial\Omega_{56}^{(i)}} \cdot \mathbf{H}_i^{(5)}(\mathbf{x}_m^{(i)}, t_{m\pm}) = H_i^{(5)}(\mathbf{x}_m^{(i)}, t_{m\pm}), \\ G^{(0,6)}_{\partial\Omega_{56}^{(i)}}(\mathbf{x}_m^{(i)}, t_{m\pm}) = \mathbf{n}^{\mathrm{T}}_{\partial\Omega_{56}^{(i)}} \cdot \mathbf{H}_i^{(6)}(\mathbf{x}_m^{(i)}, t_{m\pm}) = H_i^{(6)}(\mathbf{x}_m^{(i)}, t_{m\pm}). \end{aligned}\right\} \tag{5.21}$$

From Eqs (5.20) and (5.21), the case of (iii) holds. The other cases of (i), (ii) or (iv) can be demonstrated similarly. □

In the following theorems, the semi-passable flow's boundary motion spanning domain Ω_α and domain Ω_β is denoted by $\overrightarrow{\partial\Omega}_{\alpha\beta}$, and the first-class non-passable flow's boundary is depicted by $\widetilde{\partial\Omega}_{\alpha\beta}$.

Theorem 5.3. *(i) The sliding motion at* $\mathbf{x}_m^{(i)} \in \overrightarrow{\partial\Omega}_{12}^{(i)}$ or $\overrightarrow{\partial\Omega}_{21}^{(i)}$ $(i \in \{1,2\})$ *at time* t_m *appears if and only if*

$$\begin{aligned} &F_i^{(\beta)}(\mathbf{x}_m^{(i)}, t_{m\pm}) = 0, \ (-1)^{i+\beta} DF_i^{(\beta)}(\mathbf{x}_m^{(i)}, t_{m\pm}) > 0 \\ &\text{and } (-1)^{i+\beta} F_i^{(\alpha)}(\mathbf{x}_m^{(i)}, t_{m-}) > 0 \\ &\quad \text{for } \Omega_\alpha^{(i)} \to \widetilde{\partial\Omega}_{\alpha\beta}^{(i)}, \alpha \neq \beta \in \{1,2\}. \end{aligned} \tag{5.22}$$

(ii) The mass m_1*'s right stick-sliding motion at* $\mathbf{x}_m^{(1)} \in \overrightarrow{\partial\Omega}_{34}^{(1)}$ or $\overrightarrow{\partial\Omega}_{43}^{(1)}$ *at time* t_m *appears if and only if*

$$\begin{aligned} &F_1^{(\beta)}(\mathbf{x}_m^{(1)}, t_{m\pm}) = 0, \ (-1)^{\beta} DF_1^{(\beta)}(\mathbf{x}_m^{(1)}, t_{m\pm}) < 0 \\ &\text{and } (-1)^{\beta} F_1^{(\alpha)}(\mathbf{x}_m^{(1)}, t_{m-}) < 0 \\ &\quad \text{for } \Omega_\alpha^{(1)} \to \widetilde{\partial\Omega}_{\alpha\beta}^{(1)}, \alpha \neq \beta \in \{3,4\}. \end{aligned} \tag{5.23}$$

(iii) The mass m_1*'s left stick-sliding motion or the mass* m_2*'s stick-sliding motion at* $\mathbf{x}_m^{(i)} \in \overrightarrow{\partial\Omega}_{56}^{(i)}$ or $\overrightarrow{\partial\Omega}_{65}^{(i)}$ $(i \in \{1,2\})$ *at time* t_m *appears if and only if*

$$\begin{aligned} &H_i^{(\beta)}(\mathbf{x}_m^{(i)}, t_{m\pm}) = 0, \ (-1)^{i+\beta} DH_i^{(\beta)}(\mathbf{x}_m^{(i)}, t_{m\pm}) > 0 \\ &\text{and } (-1)^{i+\beta} H_i^{(\alpha)}(\mathbf{x}_m^{(i)}, t_{m-}) > 0 \\ &\quad \text{for } \Omega_\alpha^{(i)} \to \widetilde{\partial\Omega}_{\alpha\beta}^{(i)}, \alpha \neq \beta \in \{5,6\}. \end{aligned} \tag{5.24}$$

(iv) The mass m_1*'s double stick-sliding motion at* $\mathbf{x}_m^{(1)} \in \overrightarrow{\partial\Omega}_{78}^{(1)}$ or $\overrightarrow{\partial\Omega}_{87}^{(1)}$ *at time* t_m *appears if and only if*

$$\begin{aligned} &H_1^{(\beta)}(\mathbf{x}_m^{(1)}, t_{m\pm}) = 0, \ (-1)^{\beta} DH_1^{(\beta)}(\mathbf{x}_m^{(1)}, t_{m\pm}) < 0 \\ &\text{and } (-1)^{\beta} H_1^{(\alpha)}(\mathbf{x}_m^{(1)}, t_{m-}) < 0 \\ &\quad \text{for } \Omega_\alpha^{(1)} \to \widetilde{\partial\Omega}_{\alpha\beta}^{(1)}, \alpha \neq \beta \in \{7,8\}. \end{aligned} \tag{5.25}$$

Proof. At time t_m, based on Luo's theory of flow switchability [42], the sliding motion to appear at $\mathbf{x}_m^{(i)} \in \overrightarrow{\partial\Omega}_{21}^{(i)}$ $(i \in \{1,2\})$ satisfies the following conditions:

$$\begin{aligned} &G^{(0,1)}_{\partial\Omega_{12}^{(i)}}(\mathbf{x}_m^{(i)}, t_{m\pm}) = 0, \ (-1)^i G^{(1,1)}_{\partial\Omega_{12}^{(i)}}(\mathbf{x}_m^{(i)}, t_{m\pm}) < 0 \\ &\text{and } (-1)^i G^{(0,2)}_{\partial\Omega_{12}^{(i)}}(\mathbf{x}_m^{(i)}, t_{m-}) < 0 \\ &\quad \text{for } \Omega_2^{(i)} \to \widetilde{\partial\Omega}_{12}^{(i)}, \end{aligned} \tag{5.26}$$

Equations (5.2) and (5.4) provide

$$G^{(1,1)}_{\partial\Omega_{12}^{(i)}}(\mathbf{x}_m^{(i)}, t_{m\pm}) = \mathbf{n}^{\mathrm{T}}_{\partial\Omega_{12}^{(i)}} \cdot D\mathbf{F}_i^{(1)}(\mathbf{x}_m^{(i)}, t_{m\pm}) = DF_i^{(1)}(t_{m\pm}). \tag{5.27}$$

From Eqs (5.15), (5.26) and (5.27), the sliding motion-appearing conditions in Eq (5.22) for $\alpha = 1$ and $\beta = 2$ are established. Similar results can be derived for the other circumstances in Eqs (5.23)–(5.25). □

Theorem 5.4. *(i) The sliding motion at* $\mathbf{x}_m^{(i)} \in \widetilde{\partial\Omega}_{12}^{(i)}$ $(i \in \{1,2\})$ *at time* t_m *vanishes if and only if*

$$\left.\begin{aligned} \text{both } &(-1)^{i+\delta} F_i^{(\delta)}(\mathbf{x}_m^{(i)}, t_{m+}) > 0, \\ \text{and } &F_i^{(0>0_\delta)}(\mathbf{x}_m^{(i)}, t_{m\mp}, \tau_1^{(\delta)}) = 0 \\ \text{with } &(-1)^{i+\delta} DF_i^{(0>0_\delta)}(\mathbf{x}_m^{(i)}, t_{m\mp}, \tau_1^{(\delta)}) > 0, \\ \text{either } &(-1)^{i+\delta} F_i^{(0>0_{\bar\delta})}(\mathbf{x}_m^{(i)}, t_{m-}, \tau_1^{(\bar\delta)}) < 0 \\ \text{but } &(-1)^{i+\delta} F_i^{(\bar\delta)}(\mathbf{x}_m^{(i)}, t_{m-}) > 0, \\ \text{or } &(-1)^{i+\delta} F_i^{(0>0_{\bar\delta})}(\mathbf{x}_m^{(i)}, t_{m-}, \tau_1^{(\bar\delta)}) > 0, \\ \text{or } &F_i^{(0>0_{\bar\delta})}(\mathbf{x}_m^{(i)}, t_{m\mp}, \tau_1^{(\bar\delta)}) = 0, \\ &(-1)^{i+\delta} DF_i^{(0>0_{\bar\delta})}(\mathbf{x}_m^{(i)}, t_{m\mp}, \tau_1^{(\bar\delta)}) > 0 \end{aligned}\right\} \tag{5.28}$$

from $\widetilde{\partial\Omega}_{12}^{(i)} \to \Omega_\delta^{(i)}$*, where* $\bar\delta \neq \delta \in \{1,2\}$.

(ii) The mass m_1*'s right stick-sliding motion at* $\mathbf{x}_m^{(1)} \in \widetilde{\partial\Omega}_{34}^{(1)}$ *at time* t_m *vanishes if and only if*

$$\left.\begin{aligned} \text{both } &F_1^{(4)}(\mathbf{x}_m^{(1)}, t_{m+}) < 0, \\ \text{and } &F_1^{(0>0_4)}(\mathbf{x}_m^{(1)}, t_{m\mp}, \tau_1^{(4)}) = 0 \\ \text{with } &DF_1^{(0>0_4)}(\mathbf{x}_m^{(1)}, t_{m\mp}, \tau_1^{(4)}) < 0, \\ \text{either } &F_1^{(0>0_3)}(\mathbf{x}_m^{(1)}, t_{m-}, \tau_1^{(3)}) > 0 \\ \text{but } &F_1^{(3)}(\mathbf{x}_m^{(1)}, t_{m-}) < 0, \\ \text{or } &F_1^{(0>0_3)}(\mathbf{x}_m^{(1)}, t_{m-}, \tau_1^{(3)}) < 0, \\ \text{or } &F_1^{(0>0_3)}(\mathbf{x}_m^{(1)}, t_{m\mp}, \tau_1^{(3)}) = 0, \\ &DF_1^{(0>0_3)}(\mathbf{x}_m^{(1)}, t_{m\mp}, \tau_1^{(3)}) < 0 \end{aligned}\right\} \tag{5.29}$$

from $\widetilde{\partial\Omega}_{34}^{(1)} \to \Omega_4^{(1)}$;

$$\left.\begin{aligned} \text{both } &F_1^{(3)}(\mathbf{x}_m^{(1)}, t_{m+}) > 0, \\ \text{and } &F_1^{(0>0_3)}(\mathbf{x}_m^{(1)}, t_{m\mp}, \tau_1^{(3)}) = 0 \\ \text{with } &DF_1^{(0>0_3)}(\mathbf{x}_m^{(1)}, t_{m\mp}, \tau_1^{(3)}) > 0, \\ \text{either } &F_1^{(0>0_4)}(\mathbf{x}_m^{(1)}, t_{m-}, \tau_1^{(4)}) < 0 \\ \text{but } &F_1^{(4)}(\mathbf{x}_m^{(1)}, t_{m-}) > 0, \\ \text{or } &F_1^{(0>0_4)}(\mathbf{x}_m^{(1)}, t_{m-}, \tau_1^{(4)}) > 0, \\ \text{or } &F_1^{(0>0_4)}(\mathbf{x}_m^{(1)}, t_{m\mp}, \tau_1^{(4)}) = 0, \\ &DF_1^{(0>0_4)}(\mathbf{x}_m^{(1)}, t_{m\mp}, \tau_1^{(4)}) > 0 \end{aligned}\right\} \tag{5.30}$$

from $\widetilde{\partial\Omega}_{34}^{(1)} \to \Omega_3^{(1)}$.

(iii) The mass m_1's left stick-sliding motion or the mass m_2's stick-sliding motion at $\mathbf{x}_m^{(i)} \in \widetilde{\partial\Omega}_{56}^{(i)}$ ($i \in \{1,2\}$) at time t_m vanishes if and only if

$$\left.\begin{array}{rl}\text{both} & (-1)^{i+\delta}F_i^{(\delta)}(\mathbf{x}_m^{(i)}, t_{m+}) > 0,\\ \text{and} & F_i^{(0>0_\delta)}(\mathbf{x}_m^{(i)}, t_{m\mp}, \tau_1^{(\delta)}) = 0\\ \text{with} & (-1)^{i+\delta}DF_i^{(0>0_\delta)}(\mathbf{x}_m^{(i)}, t_{m\mp}, \tau_1^{(\delta)}) > 0,\\ \text{either} & (-1)^{i+\delta}F_i^{(0>0_{\bar\delta})}(\mathbf{x}_m^{(i)}, t_{m-}, \tau_1^{(\bar\delta)}) < 0\\ \text{but} & (-1)^{i+\delta}F_i^{(\bar\delta)}(\mathbf{x}_m^{(i)}, t_{m-}) > 0,\\ \text{or} & (-1)^{i+\delta}F_i^{(0>0_{\bar\delta})}(\mathbf{x}_m^{(i)}, t_{m-}, \tau_1^{(\bar\delta)}) > 0,\\ \text{or} & F_i^{(0>0_{\bar\delta})}(\mathbf{x}_m^{(i)}, t_{m\mp}, \tau_1^{(\bar\delta)}) = 0,\\ & (-1)^{i+\delta}DF_i^{(0>0_{\bar\delta})}(\mathbf{x}_m^{(i)}, t_{m\mp}, \tau_1^{(\bar\delta)}) > 0\end{array}\right\} \quad (5.31)$$

from $\widetilde{\partial\Omega}_{56}^{(i)} \to \Omega_\delta^{(i)}$, *where* $\bar\delta \neq \delta \in \{5,6\}$.

(iv) The mass m_1's double stick-sliding motion at $\mathbf{x}_m^{(1)} \in \widetilde{\partial\Omega}_{78}^{(1)}$ at time t_m vanishes if and only if

$$\left.\begin{array}{rl}\text{both} & H_1^{(8)}(\mathbf{x}_m^{(1)}, t_{m+}) < 0,\\ \text{and} & H_1^{(0>0_8)}(\mathbf{x}_m^{(1)}, t_{m\mp}, \tau_1^{(8)}) = 0\\ \text{with} & DF_1^{(0>0_8)}(\mathbf{x}_m^{(1)}, t_{m\mp}, \tau_1^{(8)}) < 0,\\ \text{either} & H_1^{(0>0_7)}(\mathbf{x}_m^{(1)}, t_{m-}, \tau_1^{(7)}) > 0\\ \text{but} & F_1^{(7)}(\mathbf{x}_m^{(1)}, t_{m-}) < 0,\\ \text{or} & H_1^{(0>0_7)}(\mathbf{x}_m^{(1)}, t_{m-}, \tau_1^{(7)}) < 0,\\ \text{or} & H_1^{(0>0_7)}(\mathbf{x}_m^{(1)}, t_{m\mp}, \tau_1^{(7)}) = 0,\\ & DF_1^{(0>0_7)}(\mathbf{x}_m^{(1)}, t_{m\mp}, \tau_1^{(7)}) < 0\end{array}\right\} \quad (5.32)$$

from $\widetilde{\partial\Omega}_{78}^{(1)} \to \Omega_8^{(1)}$;

$$\left.\begin{array}{rl}\text{both} & H_1^{(7)}(\mathbf{x}_m^{(1)}, t_{m+}) > 0,\\ \text{and} & H_1^{(0>0_7)}(\mathbf{x}_m^{(1)}, t_{m\mp}, \tau_1^{(7)}) = 0\\ \text{with} & DH_1^{(0>0_7)}(\mathbf{x}_m^{(1)}, t_{m\mp}, \tau_1^{(7)}) > 0,\\ \text{either} & H_1^{(0>0_8)}(\mathbf{x}_m^{(1)}, t_{m-}, \tau_1^{(8)}) < 0\\ \text{but} & H_1^{(8)}(\mathbf{x}_m^{(1)}, t_{m-}) > 0,\\ \text{or} & H_1^{(0>0_8)}(\mathbf{x}_m^{(1)}, t_{m-}, \tau_1^{(8)}) > 0,\\ \text{or} & H_1^{(0>0_8)}(\mathbf{x}_m^{(1)}, t_{m\mp}, \tau_1^{(8)}) = 0,\\ & DH_1^{(0>0_8)}(\mathbf{x}_m^{(1)}, t_{m\mp}, \tau_1^{(8)}) > 0\end{array}\right\} \quad (5.33)$$

from $\widetilde{\partial\Omega}_{78}^{(1)} \to \Omega_7^{(1)}$.

Proof. At the time t_m, the mass m_i's ($i \in \{1,2\}$) non-friction force is equivalent to the maximal static friction force, and, after time t_m, the maximal static friction force is less than the non-friction force; also, the mass m_1's left stick-sliding motion or the mass m_2's stick-sliding motion vanishes at time t_m. Based on Luo's flow switchability theory [42], the mass m_1's left stick-sliding motion vanishing at $\mathbf{x}_m^{(1)} \in \widetilde{\partial\Omega}_{56}^{(1)}$ or the mass m_2's stick-sliding motion vanishing at $\mathbf{x}_m^{(2)} \in \widetilde{\partial\Omega}_{56}^{(2)}$ with the flow barrier at time t_m satisfies the following conditions:

$$\left.\begin{array}{rl}\text{both} & (-1)^i G_{\partial\Omega_{56}^{(i)}}^{(0,6)}(\mathbf{x}_m^{(i)}, t_{m+}) > 0,\\ \text{and} & G_{\partial\Omega_{56}^{(i)}}^{(0>0_6)}(\mathbf{x}_m^{(i)}, t_{m\mp}, \tau_1^{(6)}) = 0\\ \text{with} & (-1)^i G_{\partial\Omega_{56}^{(i)}}^{(1,0>0_6)}(\mathbf{x}_m^{(i)}, t_{m\mp}, \tau_1^{(6)}) > 0,\\ \text{either} & (-1)^i G_{\partial\Omega_{56}^{(i)}}^{(0,0>0_5)}(\mathbf{x}_m^{(i)}, t_{m-}, \tau_1^{(5)}) < 0\\ \text{but} & (-1)^i G_{\partial\Omega_{56}^{(i)}}^{(0,5)}(\mathbf{x}_m^{(i)}, t_{m-}) > 0,\\ \text{or} & (-1)^i G_{\partial\Omega_{56}^{(i)}}^{(0,0>0_5)}(\mathbf{x}_m^{(i)}, t_{m-}, \tau_1^{(5)}) > 0,\\ \text{or} & G_{\partial\Omega_{56}^{(i)}}^{(0>0_5)}(\mathbf{x}_m^{(i)}, t_{m\mp}, \tau_1^{(5)}) = 0,\\ & (-1)^i G_{\partial\Omega_{56}^{(i)}}^{(1,0>0_5)}(\mathbf{x}_m^{(i)}, t_{m\mp}, \tau_1^{(5)}) > 0\end{array}\right\} \quad (5.34)$$

from $\widetilde{\partial\Omega}_{56}^{(i)} \to \Omega_6^{(i)}$;

$$\left.\begin{array}{rl}\text{both} & (-1)^i G_{\partial\Omega_{56}^{(i)}}^{(0,5)}(\mathbf{x}_m^{(i)}, t_{m+}) < 0,\\ \text{and} & G_{\partial\Omega_{56}^{(i)}}^{(0>0_5)}(\mathbf{x}_m^{(i)}, t_{m\mp}, \tau_1^{(5)}) = 0\\ \text{with} & (-1)^i G_{\partial\Omega_{56}^{(i)}}^{(1,0>0_5)}(\mathbf{x}_m^{(i)}, t_{m\mp}, \tau_1^{(5)}) < 0,\\ \text{either} & (-1)^i G_{\partial\Omega_{56}^{(i)}}^{(0,0>0_6)}(\mathbf{x}_m^{(i)}, t_{m-}, \tau_1^{(6)}) > 0\\ \text{but} & (-1)^i G_{\partial\Omega_{56}^{(i)}}^{(0,6)}(\mathbf{x}_m^{(i)}, t_{m-}) < 0,\\ \text{or} & (-1)^i G_{\partial\Omega_{56}^{(i)}}^{(0,0>0_6)}(\mathbf{x}_m^{(i)}, t_{m-}, \tau_1^{(6)}) < 0,\\ \text{or} & G_{\partial\Omega_{56}^{(i)}}^{(0>0_6)}(\mathbf{x}_m^{(i)}, t_{m\mp}, \tau_1^{(6)}) = 0,\\ & (-1)^i G_{\partial\Omega_{56}^{(i)}}^{(1,0>0_6)}(\mathbf{x}_m^{(i)}, t_{m\mp}, \tau_1^{(6)}) < 0\end{array}\right\} \quad (5.35)$$

from $\widetilde{\partial\Omega}_{56}^{(i)} \to \Omega_5^{(i)}$, where $i \in \{1,2\}$, as shown in Figure 6. Equations (4.23), (5.2) and (5.9) yield

$$\left.\begin{array}{rl} G_{\partial\Omega_{56}^{(i)}}^{(0,0>0_\delta)}(\mathbf{x}_m^{(i)}, t_{m\mp}, \tau_1^{(\delta)}) &= \mathbf{n}_{\partial\Omega_{56}^{(i)}}^{\mathrm{T}} \cdot \mathbf{H}_i^{(0>0_\delta)}(\mathbf{x}_m^{(i)}, t_{m\mp}, \tau_1^{(\delta)})\\ &= H_i^{(0>0_\delta)}(\mathbf{x}_m^{(i)}, t_{m\mp}, \tau_1^{(\delta)}),\\ G_{\partial\Omega_{56}^{(i)}}^{(1,0>0_\delta)}(\mathbf{x}_m^{(i)}, t_{m\mp}, \tau_1^{(\delta)}) &= \mathbf{n}_{\partial\Omega_{56}^{(i)}}^{\mathrm{T}} \cdot D\mathbf{H}_i^{(0>0_\delta)}(\mathbf{x}_m^{(i)}, t_{m\mp}, \tau_1^{(\delta)})\\ &= DH_i^{(0>0_\delta)}(\mathbf{x}_m^{(i)}, t_{m\mp}, \tau_1^{(\delta)}),\end{array}\right\} \quad (5.36)$$

where $\delta \in \{5,6\}$.

From Eqs (5.21) and (5.34)–(5.36), the case of (iii) holds. The other cases of (i), (ii) or (iv) can also be demonstrated in a similar manner. □

Theorem 5.5. *The grazing flow at* $\mathbf{x}_m^{(i)} \in \partial\Omega_{\alpha\beta}^{(i)}$ ($\alpha \neq \beta \in \{1,2\}$ or $\{3,4\}$ or $\{5,6\}$ or $\{7,8\}$ if $i = 1$; $\alpha \neq \beta \in$

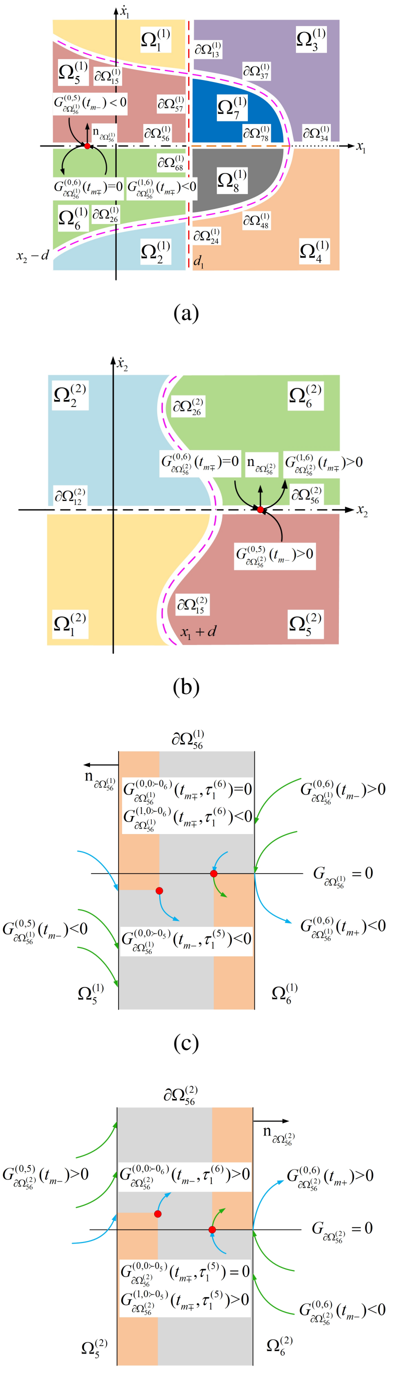

Figure 6. The left stick-sliding motion of the mass m_1 vanishes at $\mathbf{x}_m^{(1)} \in \partial\Omega_{56}^{(1)}$ or the stick-sliding motion of the mass m_2 vanishes at $\mathbf{x}_m^{(2)} \in \partial\Omega_{56}^{(2)}$ without the flow barrier for (a) mass m_1 and (b) mass m_2; the left stick-sliding motion of the mass m_1 vanishes at $\mathbf{x}_m^{(1)} \in \partial\Omega_{56}^{(1)}$ or the stick-sliding motion of the mass m_2 vanishes at $\mathbf{x}_m^{(2)} \in \partial\Omega_{56}^{(2)}$ with the flow barrier for (c) mass m_1 and (d) mass m_2.

$\{1,2\}$ or $\{5,6\}$ if $i = 2$) *at time* t_m *occurs if and only if*

$$F_i^{(\alpha)}(\mathbf{x}_m^{(i)}, t_{m\pm}) = 0 \text{ and } (-1)^{i+\alpha} DF_i^{(\alpha)}(\mathbf{x}_m^{(i)}, t_{m\pm}) > 0$$
$$\text{on } \partial\Omega_{\alpha\beta}^{(i)} \text{ in } \Omega_\alpha^{(i)}, \alpha \neq \beta \in \{1,2\} \text{ or } \{3,4\} \text{ if } i = 1;$$
$$\alpha \neq \beta \in \{1,2\} \text{ if } i = 2; \tag{5.37}$$

$$H_i^{(\alpha)}(\mathbf{x}_m^{(i)}, t_{m\pm}) = 0 \text{ and } (-1)^{i+\alpha} DH_i^{(\alpha)}(\mathbf{x}_m^{(i)}, t_{m\pm}) > 0$$
$$\text{on } \partial\Omega_{\alpha\beta}^{(i)} \text{ in } \Omega_\alpha^{(i)}, \alpha \neq \beta \in \{5,6\} \text{ or } \{7,8\} \text{ if } i = 1;$$
$$\alpha \neq \beta \in \{5,6\} \text{ if } i = 2. \tag{5.38}$$

Proof. The grazing motion happens if the object m_i's ($i \in \{1,2\}$) motion direction with reference to the ground has the same before and after time t_m, and if the object m_i's ($i \in \{1,2\}$) velocity is zero at time t_m. Based on Luo's theory of flow switchability [42], at time t_m, the grazing flow to occur at $\mathbf{x}_m^{(i)} \in \partial\Omega_{12}^{(i)}$ ($i \in \{1,2\}$) satisfies the following criteria:

$$G_{\partial\Omega_{12}^{(i)}}^{(0,1)}(\mathbf{x}_m^{(i)}, t_{m\pm}) = 0 \text{ and } (-1)^i G_{\partial\Omega_{12}^{(i)}}^{(1,1)}(\mathbf{x}_m^{(i)}, t_{m\pm}) < 0$$
$$\text{on } \partial\Omega_{12}^{(i)} \text{ in } \Omega_1^{(i)}. \tag{5.39}$$

From Eqs (5.15), (5.27) and (5.39), Eq (5.37) for $\alpha = 1$ and $\beta = 2$ is proved. The other sufficient and necessary criteria in Eqs (5.37) and (5.38) can be acquired in a comparable manner. □

5.2. At displacement boundaries in absolute coordinates

This section discusses the conditions that lead to the happening and vanishing of the mass m_1's right-only stick motion and double stick motion.

Theorem 5.6. *(i) The right-only stick motion at* $\mathbf{x}_m^{(1)} \in \partial\Omega_{13}^{(1)}$ *at time* t_m *occurs if and only if*

$$\dot{x}_1^{(1)}(\mathbf{x}_m^{(1)}, t_{m-}) > 0 \text{ and } \dot{x}_1^{(3)}(\mathbf{x}_m^{(1)}, t_{m+}) > 0$$
$$\text{for } \Omega_1^{(1)} \to \Omega_3^{(1)}. \tag{5.40}$$

(ii) The right-only stick motion at $\mathbf{x}_m^{(1)} \in \partial\Omega_{24}^{(1)}$ *at time* t_m *vanishes if and only if*

$$\dot{x}_1^{(4)}(\mathbf{x}_m^{(1)}, t_{m-}) < 0 \text{ and } \dot{x}_1^{(2)}(\mathbf{x}_m^{(1)}, t_{m+}) < 0$$
$$\text{for } \Omega_4^{(1)} \to \Omega_2^{(1)}. \tag{5.41}$$

Proof. If the mass m_1 is not touching the left damper C_3 and spring K_3 (i.e., the mass m_1 is moving freely) but the mass m_1 is touching the right spring K_6, the right stick motion occurs; when the mass m_1 is separated from the spring K_6, the right stick motion vanishes. Based on Luo's theory of flow switchability [42], the right-only stick motion that occurs at $\mathbf{x}_m^{(1)} \in \partial\Omega_{13}^{(1)}$ at time t_m satisfies the following criteria:

$$\left.\begin{array}{l} G_{\partial\Omega_{13}^{(1)}}^{(0,1)}(\mathbf{x}_m^{(1)}, t_{m-}) > 0, \\ G_{\partial\Omega_{13}^{(1)}}^{(0,3)}(\mathbf{x}_m^{(1)}, t_{m+}) > 0 \end{array}\right\} \text{ for } \Omega_1^{(1)} \to \Omega_3^{(1)}; \tag{5.42}$$

and, the right-only stick motion that vanishes at $\mathbf{x}_m^{(1)} \in \partial\Omega_{24}^{(1)}$ at time t_m satisfies the following conditions:

$$\left.\begin{array}{l} G_{\partial\Omega_{24}^{(1)}}^{(0,4)}(\mathbf{x}_m^{(1)}, t_{m-}) < 0, \\ G_{\partial\Omega_{24}^{(1)}}^{(0,2)}(\mathbf{x}_m^{(1)}, t_{m+}) < 0 \end{array}\right\} \text{ for } \Omega_4^{(1)} \to \Omega_2^{(1)}; \tag{5.43}$$

Equations (5.1) and (5.6) provide

$$\left.\begin{array}{l} G_{\partial\Omega_{13}^{(1)}}^{(0,\delta)}(\mathbf{x}_m^{(1)}, t_{m\pm}) = \mathbf{n}_{\partial\Omega_{13}^{(1)}}^{\mathrm{T}} \cdot \mathbf{F}_1^{(\delta)}(\mathbf{x}_m^{(1)}, t_{m\pm}) \\ \qquad = \dot{x}_1^{(\delta)}(\mathbf{x}_m^{(1)}, t_{m\pm}), \delta = 1, 3; \\ G_{\partial\Omega_{24}^{(1)}}^{(0,\delta)}(\mathbf{x}_m^{(1)}, t_{m\pm}) = \mathbf{n}_{\partial\Omega_{24}^{(1)}}^{\mathrm{T}} \cdot \mathbf{F}_1^{(\delta)}(\mathbf{x}_m^{(1)}, t_{m\pm}) \\ \qquad = \dot{x}_1^{(\delta)}(\mathbf{x}_m^{(1)}, t_{m\pm}), \delta = 2, 4. \end{array}\right\} \tag{5.44}$$

From Eqs (5.42)–(5.44), the cases of (i) and (ii) hold. □

Theorem 5.7. *(i) When the mass m_1 is in left stick motion, double stick motion at $\mathbf{x}_m^{(1)} \in \partial\Omega_{57}^{(1)}$ at time t_m occurs if and only if*

$$\dot{x}_1^{(5)}(\mathbf{x}_m^{(1)}, t_{m-}) > 0 \text{ and } \dot{x}_1^{(7)}(\mathbf{x}_m^{(1)}, t_{m+}) > 0 \quad \text{for } \Omega_5^{(1)} \to \Omega_7^{(1)}. \tag{5.45}$$

(ii) The mass m_1's double stick motion at $\mathbf{x}_m^{(1)} \in \partial\Omega_{68}^{(1)}$ changes to the left stick motion at time t_m if and only if

$$\dot{x}_1^{(8)}(\mathbf{x}_m^{(1)}, t_{m-}) < 0 \text{ and } \dot{x}_1^{(6)}(\mathbf{x}_m^{(1)}, t_{m+}) < 0 \quad \text{for } \Omega_8^{(1)} \to \Omega_6^{(1)}. \tag{5.46}$$

Proof. If the mass m_1 is touching the left damper C_3 and spring K_3 (i.e., the mass m_1 is in the left stick motion), the double stick motion occurs when the mass m_1 touches the right spring K_6 and they move together. When the mass m_1 is separated from the spring K_6, the mass m_1 loses double stick motion. Based on Luo's flow switchability theory [42], the double stick motion occurring at $\mathbf{x}_m^{(1)} \in \partial\Omega_{57}^{(1)}$ at time t_m satisfies the following criteria:

$$\left.\begin{array}{l} G_{\partial\Omega_{57}^{(1)}}^{(0,5)}(\mathbf{x}_m^{(1)}, t_{m-}) > 0, \\ G_{\partial\Omega_{57}^{(1)}}^{(0,7)}(\mathbf{x}_m^{(1)}, t_{m+}) > 0 \end{array}\right\} \text{ for } \Omega_5^{(1)} \to \Omega_7^{(1)}; \tag{5.47}$$

and, the criteria for the double stick motion to vanish at $\mathbf{x}_m^{(1)} \in \partial\Omega_{68}^{(1)}$ at time t_m are given by

$$\left.\begin{array}{l} G_{\partial\Omega_{68}^{(1)}}^{(0,8)}(\mathbf{x}_m^{(1)}, t_{m-}) < 0, \\ G_{\partial\Omega_{68}^{(1)}}^{(0,6)}(\mathbf{x}_m^{(1)}, t_{m+}) < 0 \end{array}\right\} \text{ for } \Omega_8^{(1)} \to \Omega_6^{(1)}. \tag{5.48}$$

One obtains the following by using Eqs (5.1) and (5.7):

$$\left.\begin{array}{l} G_{\partial\Omega_{57}^{(1)}}^{(0,\delta)}(\mathbf{x}_m^{(1)}, t_{m\pm}) = \mathbf{n}_{\partial\Omega_{57}^{(1)}}^{\mathrm{T}} \cdot \mathbf{H}_1^{(\delta)}(\mathbf{x}_m^{(1)}, t_{m\pm}) \\ \qquad = \dot{x}_1^{(\delta)}(\mathbf{x}_m^{(1)}, t_{m\pm}), \delta = 5, 7, \\ G_{\partial\Omega_{68}^{(1)}}^{(0,\delta)}(\mathbf{x}_m^{(1)}, t_{m\pm}) = \mathbf{n}_{\partial\Omega_{68}^{(1)}}^{\mathrm{T}} \cdot \mathbf{H}_1^{(\delta)}(\mathbf{x}_m^{(1)}, t_{m\pm}) \\ \qquad = \dot{x}_1^{(\delta)}(\mathbf{x}_m^{(1)}, t_{m\pm}), \delta = 6, 8. \end{array}\right\} \tag{5.49}$$

From Eqs (5.47)–(5.49), the conditions in Eqs (5.45) and (5.46) can be met, as indicated in Figure 7. □

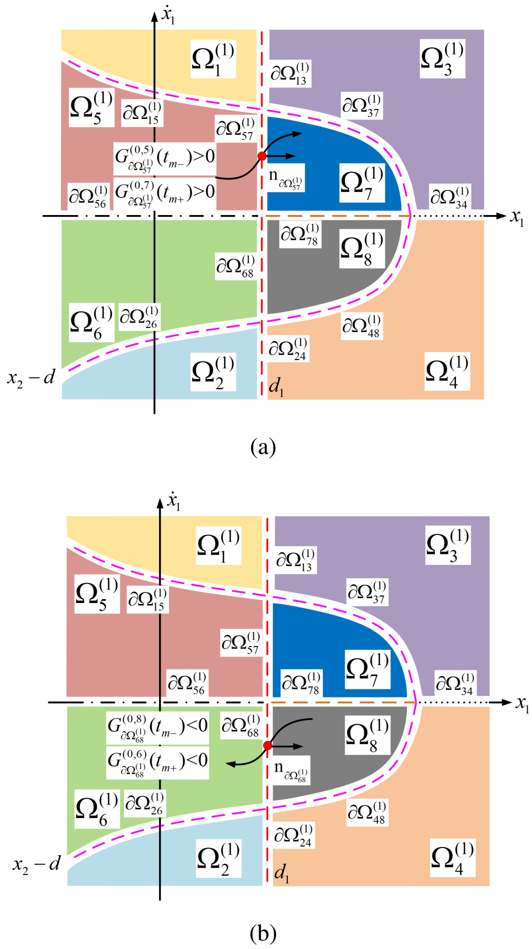

Figure 7. (a) When the mass m_1 is in left stick motion, the double stick motion occurs at $\mathbf{x}_m^{(1)} \in \partial\Omega_{57}^{(1)}$ for the mass m_1 and (b) when the mass m_1 is in left stick motion, the double stick motion vanishes at $\mathbf{x}_m^{(1)} \in \partial\Omega_{68}^{(1)}$ for the mass m_1.

5.3. At displacement boundaries in relative coordinates

This subsection includes the criteria that lead to the mass m_1's left stick motion and double stick motion occurring and disappearing in the free state or the right stick state.

Theorem 5.8. *(i) The left-only stick motion at* $\mathbf{z}_m^{(1)} \in \partial\Omega_{26}^{(1)}$ *at time* t_m *occurs if and only if*

$$\dot{z}_1^{(2)}(\mathbf{z}_m^{(1)}, t_{m-}) < 0 \text{ and } \dot{z}_1^{(6)}(\mathbf{z}_m^{(1)}, t_{m+}) < 0 \quad \text{for } \Omega_2^{(1)} \to \Omega_6^{(1)}. \tag{5.50}$$

(ii) The left-only stick motion at $\mathbf{z}_m^{(1)} \in \partial\Omega_{15}^{(1)}$ *at time* t_m *vanishes if and only if*

$$\dot{z}_1^{(5)}(\mathbf{z}_m^{(1)}, t_{m-}) > 0 \text{ and } \dot{z}_1^{(1)}(\mathbf{z}_m^{(1)}, t_{m+}) > 0 \quad \text{for } \Omega_5^{(1)} \to \Omega_1^{(1)}. \tag{5.51}$$

Proof. If the mass m_1 is not touching the spring K_6 on the right (i.e., the mass m_1 is in free-flight motion), the left stick motion occurs when the mass m_1 touches the left damper C_3 and spring K_3. When the mass m_1 is separated from the left damper C_3 and spring K_3, the mass m_1 loses the left stick motion. Based on Luo's theory of flow switchability [42], the left-only stick motion that occurs at $\mathbf{z}_m^{(1)} \in \partial\Omega_{26}^{(1)}$ at time t_m satisfies the following conditions:

$$\left.\begin{aligned} G^{(0,2)}_{\partial\Omega^{(1)}_{26}}(\mathbf{z}_m^{(1)}, t_{m-}) < 0, \\ G^{(0,6)}_{\partial\Omega^{(1)}_{26}}(\mathbf{z}_m^{(1)}, t_{m+}) < 0 \end{aligned}\right\} \quad \text{for } \Omega_2^{(1)} \to \Omega_6^{(1)}; \tag{5.52}$$

and, the left-only stick motion that vanishes at $\mathbf{z}_m^{(1)} \in \partial\Omega_{15}^{(1)}$ at time t_m satisfies the following conditions:

$$\left.\begin{aligned} G^{(0,5)}_{\partial\Omega^{(1)}_{15}}(\mathbf{z}_m^{(1)}, t_{m-}) > 0, \\ G^{(0,1)}_{\partial\Omega^{(1)}_{15}}(\mathbf{z}_m^{(1)}, t_{m+}) > 0 \end{aligned}\right\} \quad \text{for } \Omega_5^{(1)} \to \Omega_1^{(1)}. \tag{5.53}$$

Equations (5.3), (5.10) and (5.11) yield

$$\left.\begin{aligned} G^{(0,2)}_{\partial\Omega^{(1)}_{26}}(\mathbf{z}_m^{(1)}, t_{m\pm}) &= \mathbf{n}^{\mathrm{T}}_{\partial\Omega^{(1)}_{26}} \cdot \mathbf{K}_1^{(2)}(\mathbf{z}_m^{(1)}, t_{m\pm}) \\ &= \dot{z}_1^{(2)}(\mathbf{z}_m^{(1)}, t_{m\pm}), \\ G^{(0,6)}_{\partial\Omega^{(1)}_{26}}(\mathbf{z}_m^{(1)}, t_{m\pm}) &= \mathbf{n}^{\mathrm{T}}_{\partial\Omega^{(1)}_{26}} \cdot \mathbf{S}_1^{(6)}(\mathbf{z}_m^{(1)}, t_{m\pm}) \\ &= \dot{z}_1^{(6)}(\mathbf{z}_m^{(1)}, t_{m\pm}), \\ G^{(0,5)}_{\partial\Omega^{(1)}_{15}}(\mathbf{z}_m^{(1)}, t_{m\pm}) &= \mathbf{n}^{\mathrm{T}}_{\partial\Omega^{(1)}_{15}} \cdot \mathbf{S}_1^{(5)}(\mathbf{z}_m^{(1)}, t_{m\pm}) \\ &= \dot{z}_1^{(5)}(\mathbf{z}_m^{(1)}, t_{m\pm}), \\ G^{(0,1)}_{\partial\Omega^{(1)}_{15}}(\mathbf{z}_m^{(1)}, t_{m\pm}) &= \mathbf{n}^{\mathrm{T}}_{\partial\Omega^{(1)}_{15}} \cdot \mathbf{K}_1^{(1)}(\mathbf{z}_m^{(1)}, t_{m\pm}) \\ &= \dot{z}_1^{(1)}(\mathbf{z}_m^{(1)}, t_{m\pm}). \end{aligned}\right\} \tag{5.54}$$

For the mass m_1, from Eqs (5.52)–(5.54), the conditions in Eqs (5.50) and (5.51) for the occurrence and vanishment of the left-only stick motion can be acquired. □

Theorem 5.9. *(i) When the mass* m_1 *is in right stick motion, the double stick motion at* $\mathbf{z}_m^{(1)} \in \partial\Omega_{48}^{(1)}$ *at time* t_m *occurs if and only if*

$$\dot{z}_1^{(4)}(\mathbf{z}_m^{(1)}, t_{m-}) < 0 \text{ and } \dot{z}_1^{(8)}(\mathbf{z}_m^{(1)}, t_{m+}) < 0 \quad \text{for } \Omega_4^{(1)} \to \Omega_8^{(1)}. \tag{5.55}$$

(ii) The mass m_1*'s double stick motion at* $\mathbf{z}_m^{(1)} \in \partial\Omega_{37}^{(1)}$ *changes to the right stick motion at time* t_m *if and only if*

$$\dot{z}_1^{(7)}(\mathbf{z}_m^{(1)}, t_{m-}) > 0 \text{ and } \dot{z}_1^{(3)}(\mathbf{z}_m^{(1)}, t_{m+}) > 0 \quad \text{for } \Omega_7^{(1)} \to \Omega_3^{(1)}. \tag{5.56}$$

Proof. If the mass m_1 is touching the right spring K_6 (i.e., the mass m_1 is in the right stick motion), and the mass m_1 touches the left damper C_3 and spring K_3, the double stick motion happens. When the mass m_1 is separated from the left damper C_3 and spring K_3, the mass m_1 loses the double stick motion. Based on Luo's flow switchability theory [42], the double stick motion that occurs at $\mathbf{z}_m^{(1)} \in \partial\Omega_{48}^{(1)}$ at time t_m satisfies the following criteria:

$$\left.\begin{aligned} G^{(0,4)}_{\partial\Omega^{(1)}_{48}}(\mathbf{z}_m^{(1)}, t_{m-}) < 0, \\ G^{(0,8)}_{\partial\Omega^{(1)}_{48}}(\mathbf{z}_m^{(1)}, t_{m+}) < 0 \end{aligned}\right\} \quad \text{for } \Omega_4^{(1)} \to \Omega_8^{(1)}; \tag{5.57}$$

and the double stick motion that vanishes at $\mathbf{z}_m^{(1)} \in \partial\Omega_{37}^{(1)}$ at time t_m satisfies the following criteria:

$$\left.\begin{aligned} G^{(0,7)}_{\partial\Omega^{(1)}_{37}}(\mathbf{z}_m^{(1)}, t_{m-}) > 0, \\ G^{(0,3)}_{\partial\Omega^{(1)}_{37}}(\mathbf{z}_m^{(1)}, t_{m+}) > 0 \end{aligned}\right\} \quad \text{for } \Omega_7^{(1)} \to \Omega_3^{(1)}, \tag{5.58}$$

as demonstrated in Figure 8. Equations (5.3), (5.10) and (5.11) yield

$$\left.\begin{aligned} G^{(0,4)}_{\partial\Omega^{(1)}_{48}}(\mathbf{z}_m^{(1)}, t_{m\pm}) &= \mathbf{n}^{\mathrm{T}}_{\partial\Omega^{(1)}_{48}} \cdot \mathbf{K}_1^{(4)}(\mathbf{z}_m^{(1)}, t_{m\pm}) \\ &= \dot{z}_1^{(4)}(\mathbf{z}_m^{(1)}, t_{m\pm}), \\ G^{(0,8)}_{\partial\Omega^{(1)}_{48}}(\mathbf{z}_m^{(1)}, t_{m\pm}) &= \mathbf{n}^{\mathrm{T}}_{\partial\Omega^{(1)}_{48}} \cdot \mathbf{S}_1^{(8)}(\mathbf{z}_m^{(1)}, t_{m\pm}) \\ &= \dot{z}_1^{(8)}(\mathbf{z}_m^{(1)}, t_{m\pm}), \\ G^{(0,7)}_{\partial\Omega^{(1)}_{37}}(\mathbf{z}_m^{(1)}, t_{m\pm}) &= \mathbf{n}^{\mathrm{T}}_{\partial\Omega^{(1)}_{37}} \cdot \mathbf{S}_1^{(7)}(\mathbf{z}_m^{(1)}, t_{m\pm}) \\ &= \dot{z}_1^{(7)}(\mathbf{z}_m^{(1)}, t_{m\pm}), \\ G^{(0,3)}_{\partial\Omega^{(1)}_{37}}(\mathbf{z}_m^{(1)}, t_{m\pm}) &= \mathbf{n}^{\mathrm{T}}_{\partial\Omega^{(1)}_{37}} \cdot \mathbf{K}_1^{(3)}(\mathbf{z}_m^{(1)}, t_{m\pm}) \\ &= \dot{z}_1^{(3)}(\mathbf{z}_m^{(1)}, t_{m\pm}). \end{aligned}\right\} \tag{5.59}$$

From Eqs (5.57)–(5.59), the cases of (i) and (ii) hold. □

Remark 5.1. *Similar to the geometric diagrams for the analytic conditions for Theorems 5.4, 5.7 and 5.9, the geometric diagrams for the analytic conditions for other theorems can also be drawn.*

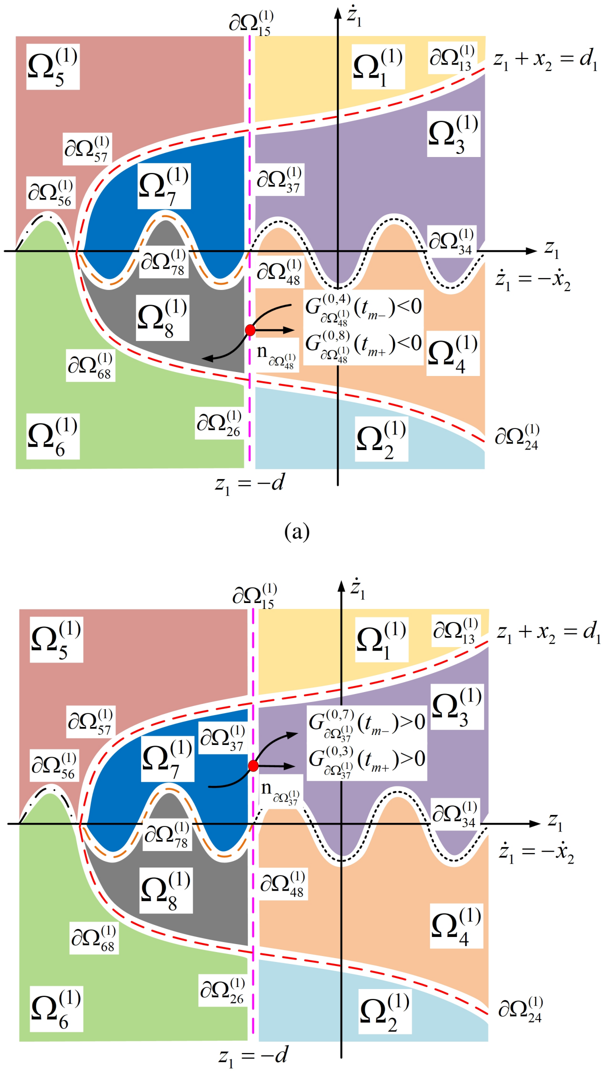

(a)

(b)

Figure 8. (a) When the mass m_1 is in right stick motion, the double stick motion occurs at $\partial\Omega^{(1)}_{48}$ for the mass m_1 and (b) the mass m_1's double stick motion changes to the right stick motion.

6. Numerical simulations

Numerical simulations of the sliding, grazing, left stick and periodic motions are illustrated in Figures 9–13, respectively, to help better understand the discontinuous dynamical system's switching conditions in this paper. Figures 9a–13a describe the displacement versus time curves; the velocity versus time curves are represented by Figures 9b–13b; the phase space trajectories are demonstrated in Figures 9c–13c; Figures 9d–13d display the G-function versus time histories. In Figures 9–13, green-filled circles serve as representations of the movement starting points of the masses m_1 and m_2. Additionally, yellow-, white- and red-filled circles are used to illustrate the switching spots. The black and blue dashed lines show the velocity boundaries; the red dashed lines can be seen as the displacement boundaries; the blue and black solid curves respectively illustrate how the objects m_1 and m_2 moved. In Figures 9d–13d, the solid and dashed curves respectively depict the objects m_1's and m_2's real and imaginary responses to forces, and the differently colored curves depict the forces influencing the objects m_1 and m_2 in various domains.

Instance 1 (Sliding motion): Based on a set of system parameters $m_1 = 1$ kg, $m_2 = 1$ kg, $C_1 = 0.05$ N·s/m, $C_2 = 0.05$ N·s^3/m^3, $C_3 = 1$ N·s/m, $C_4 = 0.05$ N·s/m, $C_5 = 0.05$ N·s^3/m^3, $K_1 = 0.6$ N/m, $K_2 = 1$ N/m^3, $K_3 = 2$ N/m, $K_4 = 1.5$ N/m, $K_5 = 1$ N/m^3, $K_6 = 1$ N/m, $\mu_k = 0.1$, $\mu_s = 0.2$, $d = 5$ m, $d_1 = 4.5$ m, $Q_1 = 30$ N, $Q_2 = 71$ N, $\varphi_1 = \varphi_2 = 0$ rad, $P_1 = P_2 = \pi/8$ N, $\Omega = 1.6$ rad/s and $g = 9.8$ m/s^2 and initial states of $t_0 = 1$ s, $\dot{x}_1 = 0$ m/s, $x_1 = 3$ m, $\dot{x}_2 = 0$ m/s and $x_2 = 4$ m, Figure 9 depicts the objects m_1's and m_2's sliding motion. The shaded part denotes that the object m_1 or the object m_2 is performing a sliding motion. It is observed in Figure 9b that, at the initial time $t_0 = 1$ s, the masses m_1 and m_2 move at a constant speed of zero, and Figure 9d shows the forces $F^{(1)}_2 > 0$ and $F^{(2)}_2 < 0$, which means that Theorem 5.2's Eq (5.16) is satisfied. Because the velocity boundary $\partial\Omega^{(2)}_{12}$ has flow barriers, within the time interval (1 s, 1.1749 s), the displacement of the mass m_2 does not change. At time $t_1 = 1.1749$ s, according to the force $F^{(0\succ 0_1)}_2$ in Figure 9d, we obtain the first-order G-function $DF^{(0\succ 0_1)}_2 < 0$, and there are the forces $F^{(1)}_2 < 0$, $F^{(0\succ 0_2)}_2 < 0$ and $F^{(0\succ 0_1)}_2 = 0$, which satisfy the conditions of Eq (5.28) in Theorem 5.4 for sliding motion disappearing for the mass m_2; thus, the object m_2 will move out of the velocity boundary and enter the domain $\Omega^{(2)}_1$. According to Figure 9b, the mass m_2 is free to travel throughout the domain $\Omega^{(2)}_1$ during the time window (1.1749 s, 1.9 s). In addition, similar to the mass m_2's analysis method, the object m_1 makes the sliding motion in the time interval (1 s, 1.2821 s). At time $t_2 = 1.2821$ s, the object m_1 will move out of

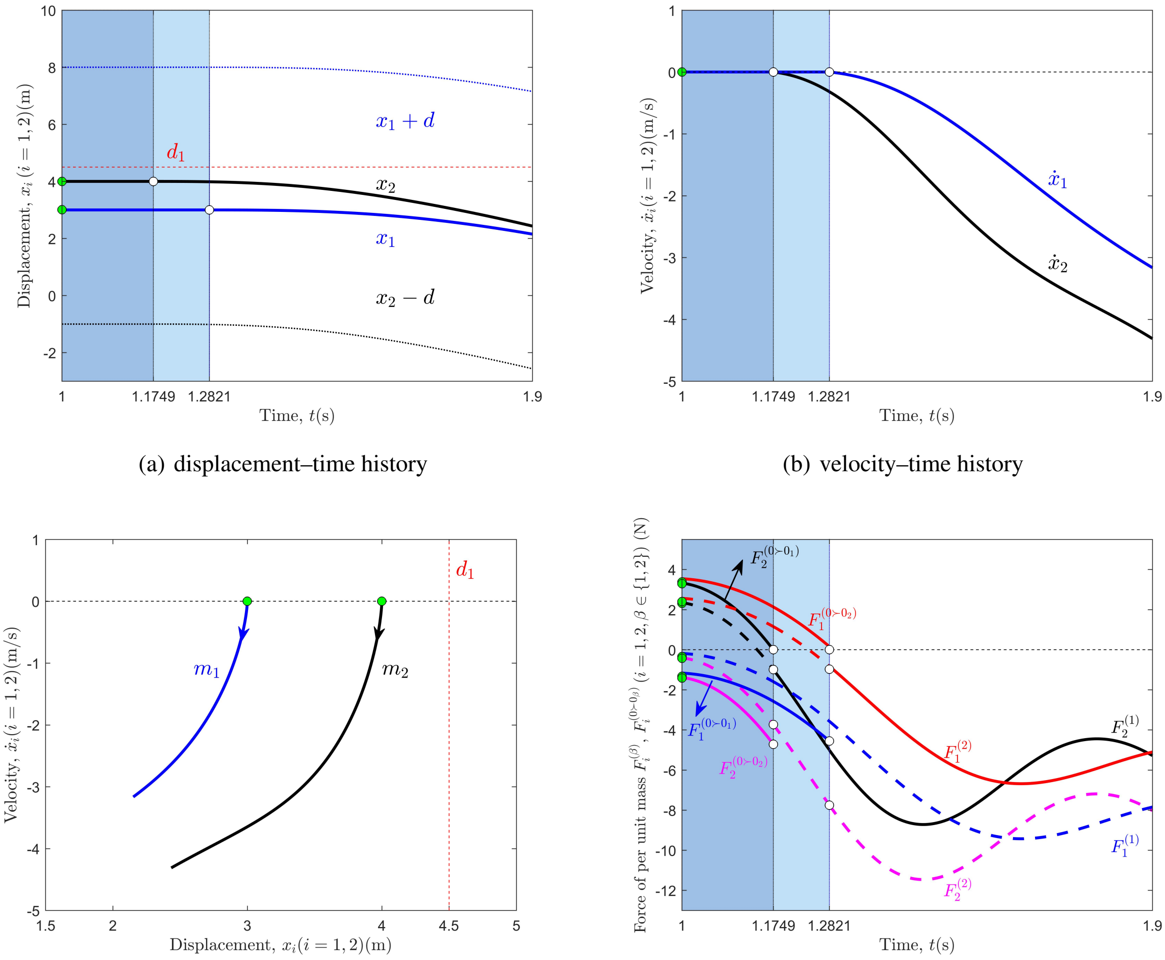

(a) displacement–time history

(b) velocity–time history

(c) phase trajectory

(d) force per unit mass versus time history

Figure 9. Instance 1 simulation of sliding motion for the masses m_1 and m_2.

the boundary $\partial\Omega_{12}^{(1)}$; during the time interval (1.2821 s, 1.9 s) shown in Figure 9b, the mass m_1 is free to travel throughout the domain $\Omega_2^{(1)}$.

Instance 2 (Grazing motion): To demonstrate that the mass m_2 is performing the grazing motion at the boundary $\partial\Omega_{12}^{(2)}$, the parameters of the system were chosen as $m_1 = 1$ kg, $m_2 = 1$ kg, $C_1 = 0.05$ N·s/m, $C_2 = 0.05$ N·s^3/m^3, $C_3 = 1$ N·s/m, $C_4 = 0.05$ N·s/m, $C_5 = 0.05$ N·s^3/m^3, $K_1 = 1$ N/m, $K_2 = 1$ N/m^3, $K_3 = 2$ N/m, $K_4 = 1$ N/m, $K_5 = 1$ N/m^3, $K_6 = 1$ N/m, $\mu_k = 0.15$, $\mu_s = 0.2$, $d = 4$ m, $d_1 = 3$ m, $Q_1 = 10$ N, $Q_2 = 10$ N, $\varphi_1 = \varphi_2 = 0$ rad, $P_1 = P_2 = \pi/30$ N, $\Omega = 2.6$ rad/s and $g = 9.8$ m/s^2, and the initial conditions were selected as $t_0 = 3$ s, $\dot{x}_1 = 3$ m/s, $x_1 = 2$ m, $\dot{x}_2 = -10$ m/s and $x_2 = 1$ m. During the time window (3 s, 3.813 s), the mass m_2 is free to travel throughout the domain $\Omega_1^{(2)}$, and, at the instant $t_1 = 3.813$ s, it reaches the boundary $\partial\Omega_{12}^{(2)}$, as observed in Figure 10b. Figure 10d demonstrates that there is $F_2^{(1)} = 0$, and, according to the slope of the curve of the force $F_2^{(1)}$, at time t_1, we obtain the first-order G-function $DF_2^{(1)} < 0$, which satisfies Eq (5.37) in Theorem 5.5. In other words, the mass m_2 is performing grazing motion at time t_1. After $t_1 = 3.813$ s, the mass m_2 returns to the domain $\Omega_1^{(2)}$ and continues to perform free motion until time $t_2 = 4.5$ s in Figure 10b. During the time window (3 s, 3.325 s), the mass m_1 is free to travel in the domain $\Omega_1^{(1)}$. According to Eq (5.12) in Theorem 5.1 and the forces $F_1^{(1)} < 0$ and $F_1^{(2)} < 0$ plotted in Figure 10d, the mass m_1 will move out of the boundary $\partial\Omega_{12}^{(1)}$ and into the domain $\Omega_2^{(1)}$ at $t = 3.325$ s.

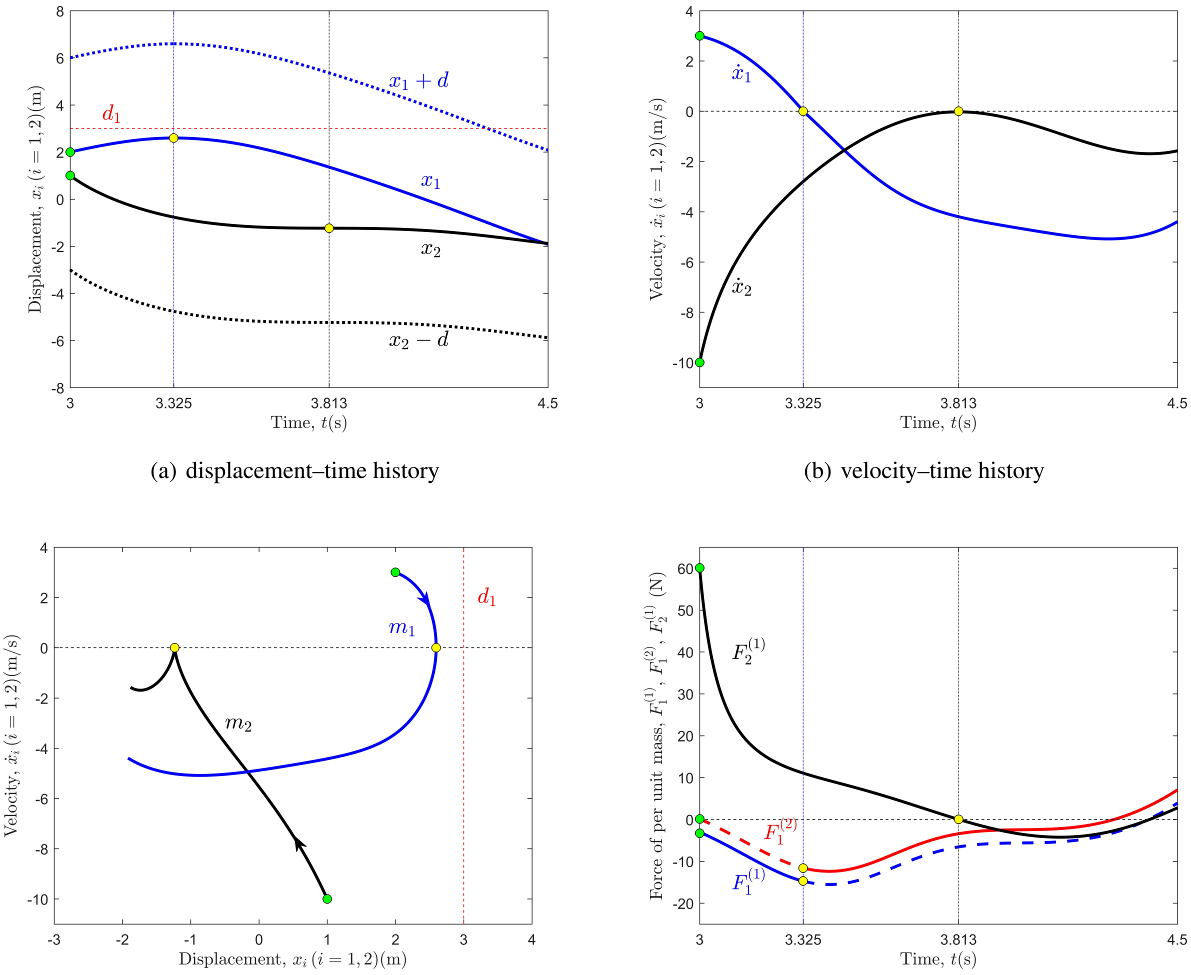

(a) displacement–time history

(b) velocity–time history

(c) phase trajectory

(d) force per unit mass versus time history

Figure 10. Instance 2 simulation of grazing motion for the mass m_2.

Until $t_4 = 4.5$ s, the object m_1 continues to travel about the domain $\Omega_2^{(1)}$.

Instance 3 (Left stick motion): Select a set of system parameters $m_1 = 2$ kg, $m_2 = 2$ kg, $C_1 = 0.05$ N·s/m, $C_2 = 0.05$ N·s^3/m^3, $C_3 = 1$ N·s/m, $C_4 = 1$ N·s/m, $C_5 = 0.05$ N·s^3/m^3, $K_1 = 1$ N/m, $K_2 = 1$ N/m^3, $K_3 = 2$ N/m, $K_4 = 3$ N/m, $K_5 = 2$ N/m^3, $K_6 = 1$ N/m, $\mu_k = 0.2$, $\mu_s = 0.25$, $d = 1.5$ m, $d_1 = 5.5$ m, $Q_1 = 16$ N, $Q_2 = 25$ N, $\varphi_1 = \varphi_2 = 0$ rad, $P_1 = P_2 = \pi/6$ N, $\Omega = 2.6$ rad/s and $g = 9.8$ m/s^2 and initial conditions of $t_0 = 1.5$ s, $\dot{x}_1 = 2$ m/s, $x_1 = 3.5$ m, $\dot{x}_2 = -1$ m/s and $x_2 = 3$ m to illustrate the mass m_1's left stick motion in Figure 11. According to Figure 11a, in the time interval (1.5 s, 3.0215 s), the difference in displacement $x_1 - x_2 > -d$ indicates that the objects m_1 and m_2 are in free motion. Figure 11b illustrates that the mass m_1 enters into the domain $\Omega_2^{(1)}$ at $t = 1.5622$ s; then, the mass m_1 enters into the domain $\Omega_1^{(1)}$ at $t = 2.8501$ s. At $t = 2.5471$ s, the mass m_2 can enter into the domain $\Omega_2^{(2)}$ via the boundary $\partial\Omega_{12}^{(2)}$. Figure 11a,c demonstrates, with a relative velocity of $\dot{x}_1 - \dot{x}_2 < 0$, that the mass m_1 arrives at the displacement boundary at $t_1 = 3.0215$ s. Therefore, the conditions of Eq (5.50) of Theorem 5.8 are met, so the mass m_1 enters the left stick domain. In the time interval (3.0251 s, 3.7786 s), the left stick-nonsliding motion is performed by the mass m_1, whereas the stick-nonsliding motion is performed by the mass m_2. At the switching time $t_2 = 3.7786$ s, the objects m_1 and m_2 enter the free domains in accordance with Eq (5.51) in Theorem 5.8 and $\dot{x}_1 - \dot{x}_2 > 0$, as shown in Figure 11c.

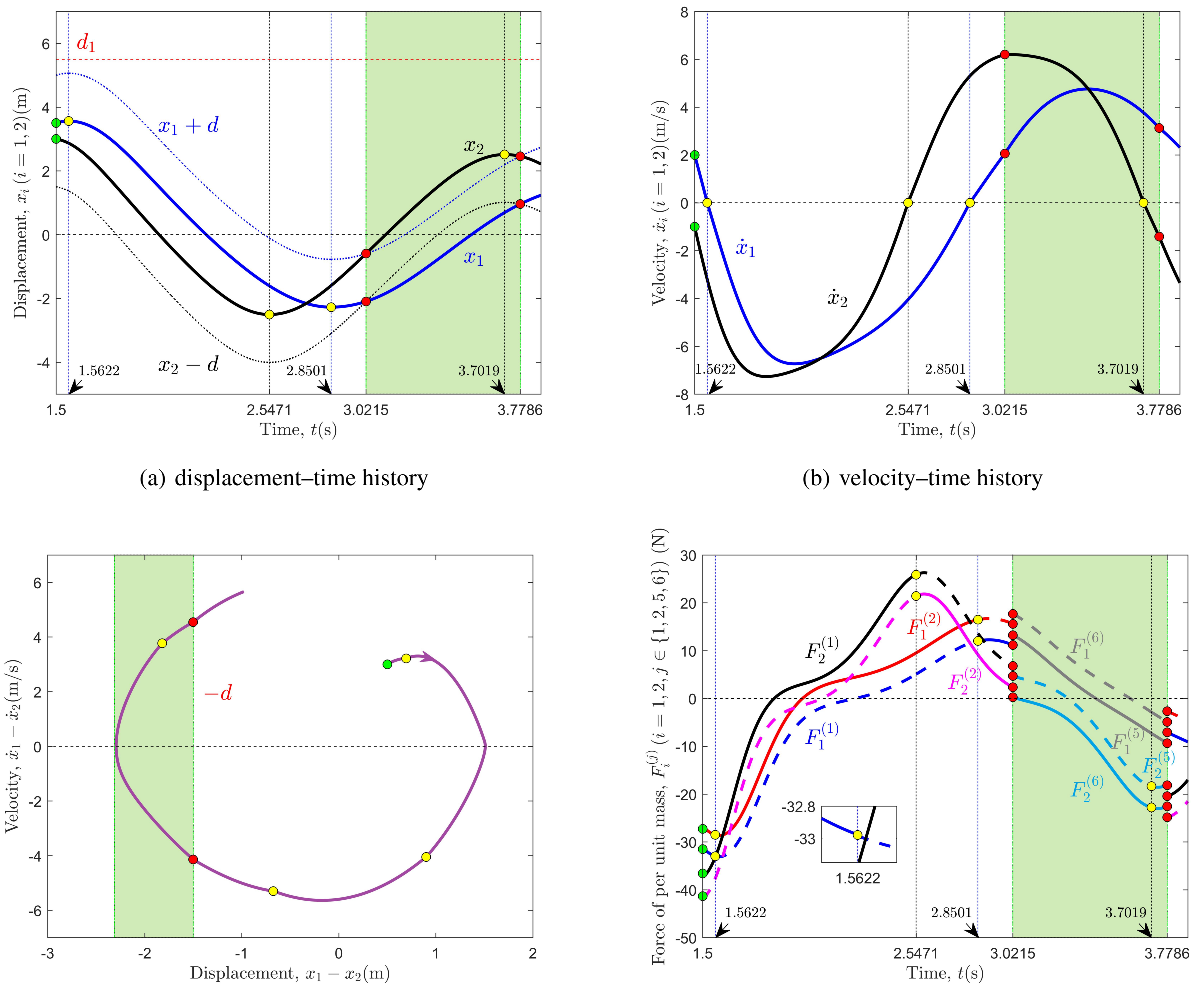

(a) displacement–time history (b) velocity–time history

(c) phase trajectory (d) force per unit mass versus time history

Figure 11. Instance 3 simulation of left stick motion for the mass m_1.

In addition, the object m_2 completes a passable motion in the stick motion's process at $t = 3.7019$ s; it is shown in Figure 11b.

Instance 4 (Passable periodic motion): Using a set of parameters $m_1 = 1$ kg, $m_2 = 1$ kg, $C_1 = 0.05$ N·s/m, $C_2 = 0.05$ N·s^3/m^3, $C_3 = 1$ N·s/m, $C_4 = 2$ N·s/m, $C_5 = 0.05$ N·s^3/m^3, $K_1 = 1$ N/m, $K_2 = 1$ N/m^3, $K_3 = 2$ N/m, $K_4 = 1$ N/m, $K_5 = 1$ N/m^3, $K_6 = 1$ N/m, $\mu_k = 0.2$, $\mu_s = 0.26$, $d = 4.5$ m, $d_1 = 4$ m, $Q_1 = 12.3268$ N, $Q_2 = 17$ N, $\varphi_1 = \pi$ rad, $\varphi_2 = 0$ rad, $P_1 = P_2 = \pi/3$ N, $\Omega = 2.6$ rad/s and $g = 9.8$ m/s^2 and initial conditions of $t_0 = 1.3322$ s, $\dot{x}_1 = 0$ m/s, $x_1 = -2.3661$ m, $\dot{x}_2 = 0$ m/s and $x_2 = 1.7095$ m, Figure 12 illustrates the objects m_1's and m_2's passable periodic motion. At $t_0 = 1.3322$ s, the object m_1 is at the boundary $\partial\Omega_{12}^{(1)}$ and the object m_2 is at the boundary $\partial\Omega_{12}^{(2)}$, as shown in Figure 12b,c, respectively. As exhibited in Figure 12d, there are the forces $F_2^{(1)} < 0$ and $F_2^{(2)} < 0$ at time t_0; according to Theorem 5.1's Eq (5.12), the mass m_2 enters the domain $\Omega_1^{(2)}$. During the time window (1.3322 s, 2.5402 s), the mass m_2 is free to travel throughout the domain $\Omega_1^{(2)}$. At $t_1 = 2.5402$ s, the mass m_2 arrives at the velocity boundary $\partial\Omega_{12}^{(2)}$, and in Figure 12b,d, as a result of the forces $F_2^{(1)} > 0$ and $F_2^{(2)} > 0$, the mass m_2 launches into the domain $\Omega_2^{(2)}$. During the time window (2.5402 s, 3.7485 s), the mass m_2 is free to travel in the domain $\Omega_2^{(2)}$. Figure 12a,b illustrate that, at time $t_2 = 3.7485$ s, the mass

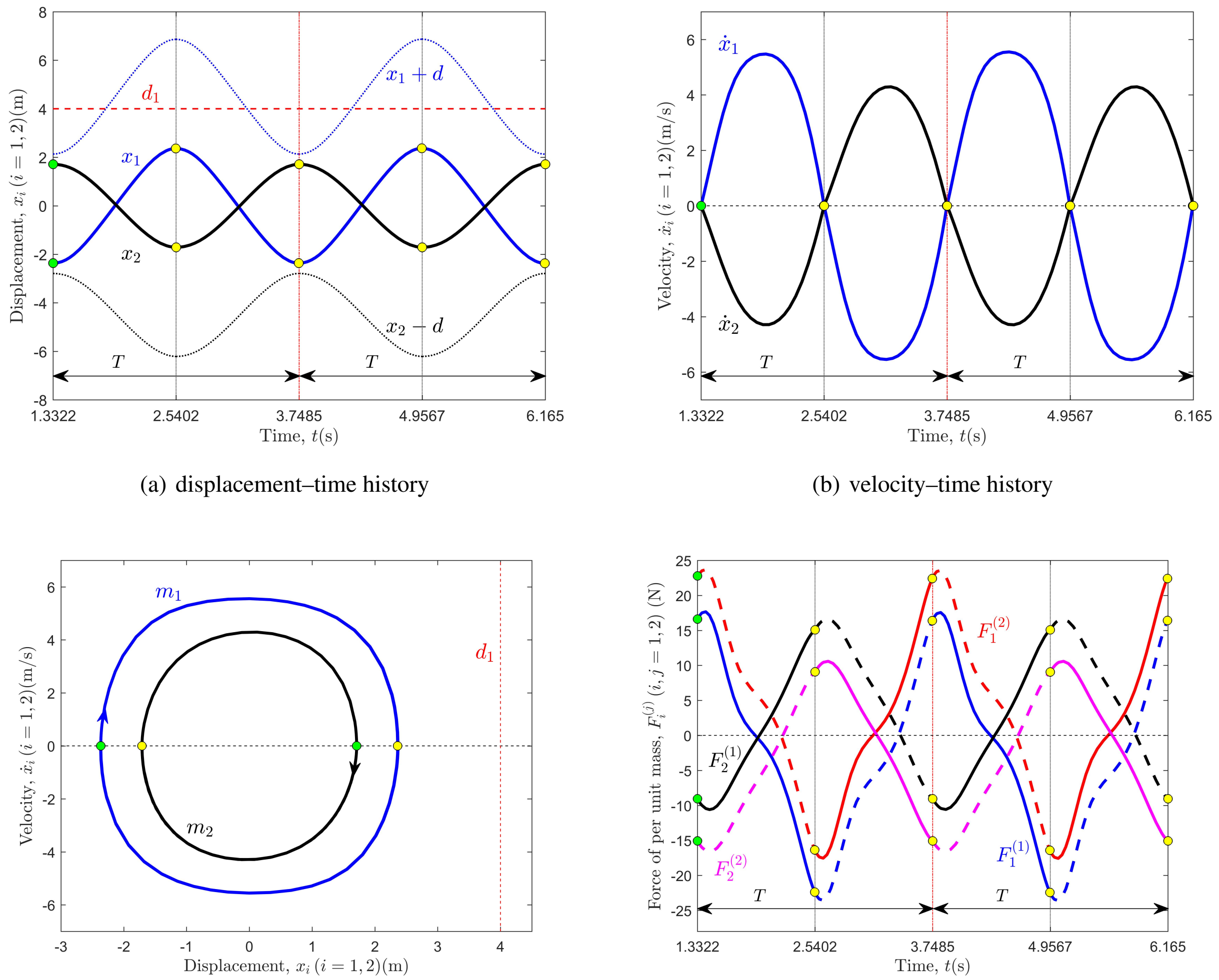

(a) displacement–time history

(b) velocity–time history

(c) phase trajectory

(d) force per unit mass versus time history

Figure 12. Instance 4 simulation of passable periodic motion for the masses m_1 and m_2.

m_2 returns to the starting location. Similar to the motion of the mass m_2, at $t_0 = 1.3322$ s, the mass m_1 will enter $\Omega_1^{(1)}$ owing to the forces $F_1^{(1)} > 0$ and $F_1^{(2)} > 0$ in Figure 12d and Theorem 5.1's Eq (5.12); thus, the mass m_1 is free to wander around the domain $\Omega_1^{(1)}$; then, the mass m_1 goes across the boundary $\partial\Omega_{12}^{(1)}$ to the domain $\Omega_2^{(1)}$ and returns to the original position. After that, the masses m_1 and m_2 begin the second period.

Instance 5 (Right-stick periodic motion): As illustrated in Figure 13, we selected the parameters $m_1 = 1.021$ kg, $m_2 = 1$ kg, $C_1 = 0.05$ N·s/m, $C_2 = 0.05$ N·s^3/m^3, $C_3 = 1$ N·s/m, $C_4 = 2$ N·s/m, $C_5 = 0.05$ N·s^3/m^3, $K_1 = 1$ N/m, $K_2 = 1$ N/m^3, $K_3 = 2$ N/m, $K_4 = 1$ N/m, $K_5 = 1$ N/m^3, $K_6 = 1$ N/m, $\mu_k = 0.2$, $\mu_s = 0.25$, $d = 4.5$ m, $d_1 = 1.8$ m, $Q_1 = 12.39$ N, $Q_2 = 17$ N, $\varphi_1 = \pi$ rad, $\varphi_2 = 0$ rad, $P_1 = P_2 = \pi/3$ N, $\Omega = 2.6$ rad/s and $g = 9.8$ m/s^2 and initial conditions of $t_0 = 1.3322$ s, $\dot{x}_1 = 0$ m/s, $x_1 = -2.3724$ m, $\dot{x}_2 = 0$ m/s and $x_2 = 1.7096$ m to account for the mass m_1's right-stick periodic motion. As exhibited in Figure 13b, at the initial moment $t_0 = 1.3322$ s, the objects m_1 and m_2 are both at the boundaries $\partial\Omega_{12}^{(1)}$ and $\partial\Omega_{12}^{(2)}$, respectively. The object m_1 will launch into the domain $\Omega_1^{(1)}$ at the initial moment according to Eq (5.12) in Theorem 5.1 and the forces $F_1^{(1)} > 0$ and $F_1^{(2)} > 0$ in Figure 13d. As shown in Figure 13a, during the time window (1.3322 s, 2.2966 s), the mass m_1 is free to travel throughout the domain $\Omega_1^{(1)}$ until the mass m_1 reaches the displacement boundary $\partial\Omega_{13}^{(1)}$. Considering this with Figure 13b, the mass m_1 is moving at a velocity that is

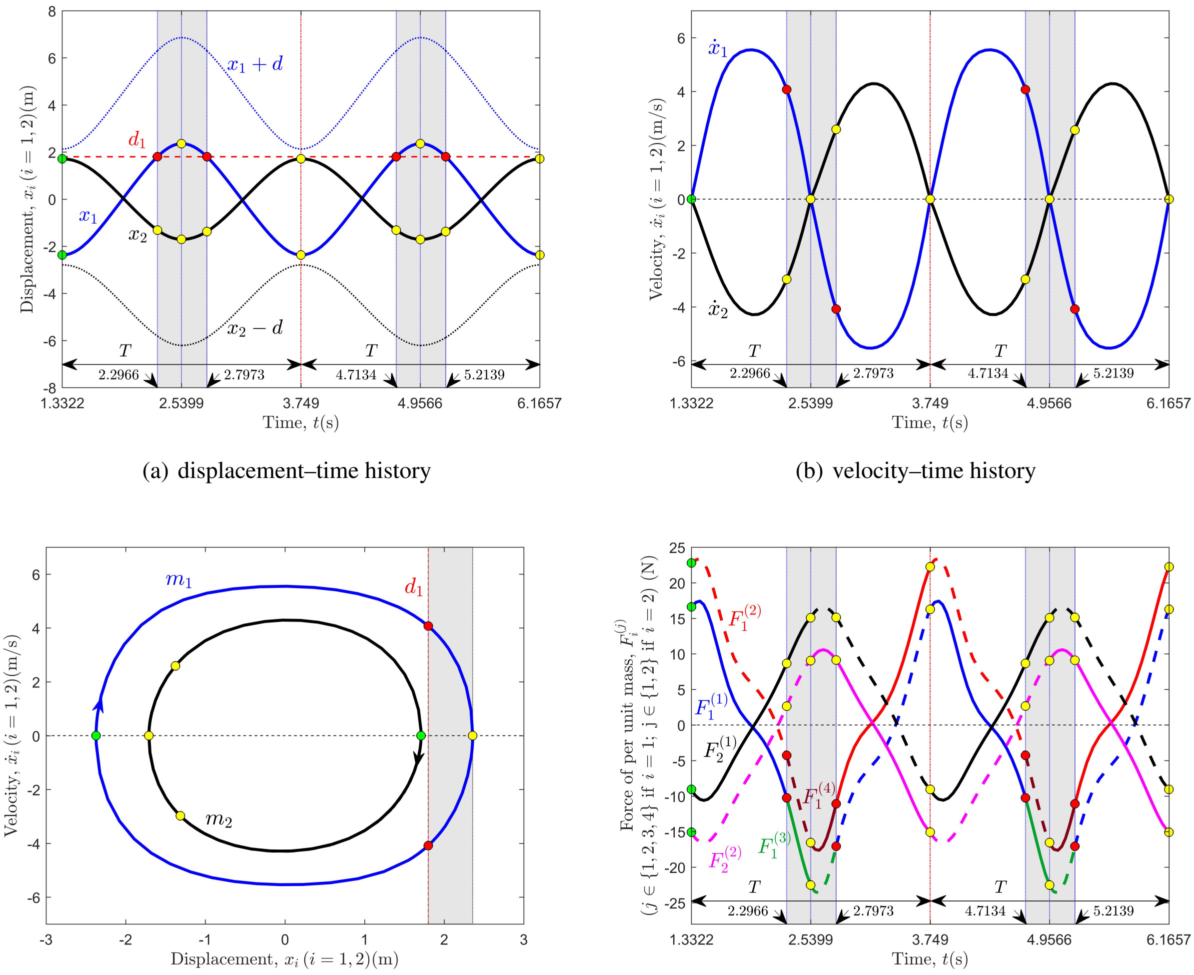

(a) displacement–time history

(b) velocity–time history

(c) phase trajectory

(d) force per unit mass versus time history

Figure 13. Instance 5 simulation of right-stick periodic motion for the mass m_1.

greater than zero, so the criteria in Eq (5.40) of Theorem 5.6 for the occurrence of the right-stick motion are met. Therefore, within the time interval (2.2966 s, 2.5399 s), in the domain $\Omega_3^{(1)}$, the mass m_1 exhibits right-stick nonsliding motion. At the time $t_2 = 2.5399$ s, there are forces $F_1^{(3)} < 0$ and $F_1^{(4)} < 0$ in Figure 13d that satisfy the conditions of Theorem 5.1's Eq (5.12); thus, the object m_1 crosses the boundary $\partial\Omega_{34}^{(1)}$ and into the domain $\Omega_4^{(1)}$. During a certain time (2.5399 s, 2.7973 s), the object m_1 is free to travel throughout $\Omega_4^{(1)}$ in Figure 13b. At $t_3 = 2.7973$ s, the mass m_1 leaves displacement boundary $\partial\Omega_{24}^{(1)}$ since its velocity is less than zero according to Figure 13b and Eq (5.41) of Theorem 5.6. Therefore, the mass m_1 is free to travel throughout the domain $\Omega_2^{(1)}$ during the time window (2.7973 s, 3.7490 s). At the time $t_4 = 3.7490$ s, the second period is initiated when the mass m_1 returns to the starting location. While the object m_1 conducts the right-stick periodic motion, the object m_2 performs passable periodic motion.

7. Scene of sliding bifurcation

In nonlinear dynamical systems, the sliding bifurcation may lead to a change in the topology of the steady-state solution of the system, which has a significant impact on the system's dynamical behavior. Studying sliding bifurcation will help one to better analyze the stability of the system's periodic motion, and this section will give the object m_2's sliding bifurcation at the velocity boundary $\partial\Omega_{12}^{(2)}$ for the excitation amplitude and frequency.

We chose the parameters $m_1 = 1$ kg, $m_2 = 1$ kg, $C_1 = 0.05$ N·s/m, $C_2 = 0.05$ N·s^3/m^3, $C_3 = 1$ N·s/m, $C_4 = 0.05$ N·s/m, $C_5 = 0.05$ N·s^3/m^3, $K_1 = 0.6$ N/m, $K_2 = 1$ N/m^3, $K_3 = 2$ N/m, $K_4 = 1.5$ N/m, $K_5 = 1$ N/m^3, $K_6 = 1$ N/m, $\mu_k = 0.1$, $\mu_s = 0.2$, $d = 5$ m, $d_1 = 4.5$ m, $Q_1 = 30$ N, $\varphi_1 = \varphi_2 = 0$ rad, $P_1 = P_2 = \pi/8$ N and $g = 9.8$ m/s^2. Using Theorem 5.2, when $Q_2 = 71$ N and Ω is in the range of $[1.3, 1.85]$, the object m_2's sliding bifurcation for the excitation frequency is as depicted in Figure 14a. In addition, Figure 14b depicts the sliding bifurcation of the object m_2 for the excitation amplitude within the region of $Q_2 \in [68.5, 72]$ and $\Omega = 1.6$ rad/s.

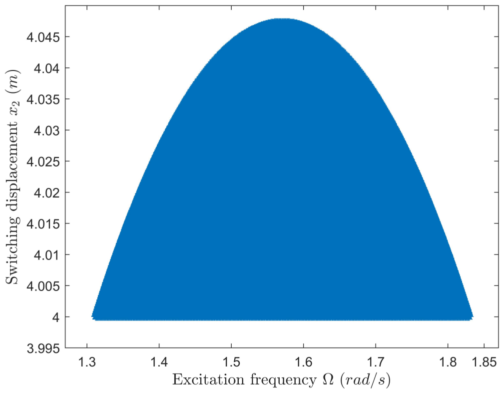

(a)

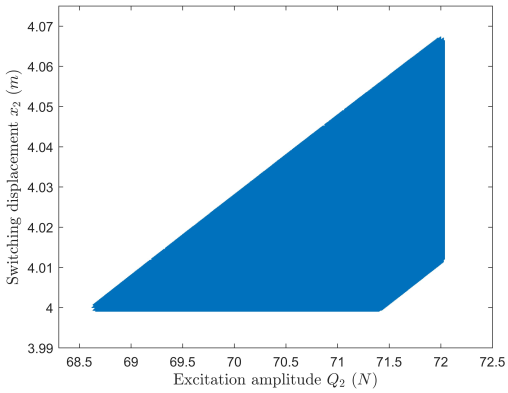

(b)

Figure 14. Sliding bifurcation scenario at the velocity boundary $\partial\Omega_{12}^{(2)}$ for the mass m_2: (a) varying the excitation frequency Ω and (b) varying the excitation amplitude Q_2.

8. Conclusions

In this paper, we have investigated the discontinuous dynamical behaviors of a class of 2-DOF systems, where such a system has asymmetric elastic constraints. Due to collision and friction, the dynamic system is nonsmooth at the displacement boundary and discontinuous at the velocity boundary. Under the condition of the nonsmoothness and discontinuities, to specify a continuous dynamical system in each domain, the phase plane of the oscillator was divided into various boundaries and domains. The 2-DOF frictional vibration system's switchability and local singularity of flows to the dynamic boundaries have been explored in depth; additionally, by using the flow switching theory for discontinuous dynamical systems, we have analyzed the switching criteria for typical motions at the separation boundary in this work. Additionally, numerical simulations of many typical motions were performed to show how the motion of the object varies at the nonsmooth or discontinuous boundary, and the object sliding bifurcation scene is depicted in this paper. These results help us to better understand such 2-DOF system's complex dynamic behaviors.

The 2-DOF system possesses the following features:

(i) The cushioning functions of the linear and nonlinear dampers and the linear and nonlinear springs are considered.

(ii) The negative feedback acting on the object depends on the velocity of the object, which has more applications in reality.

(iii) The system has different static and kinetic friction forces, which causes flow barriers to exist.

(iv) Since two objects can interact with each other through a spring and damper, the system's motion states are more intricate.

Through rigorous mathematical analysis, we have aimed to provide a thorough and original exploration of the discontinuous dynamics for a class of 2-DOF frictional vibration systems with asymmetric elastic constraints; it might deepen our comprehension of the 2-DOF system. Vibro-impact systems can be seen in the industry, imcluding in impact vibration rollers, impact vibration dampers, vibration conveyors, etc. Therefore, studying the dynamic properties of a vibration system where friction and elastic collision coexist is extremely important to reveal the consequences of elastic collision. The results of this paper can provide some theoretical references for the mechanical systems with asymmetric elastic constraints, dynamic parameter optimization and noise reduction.

Use of AI tools declaration

The authors declare they have not used Artificial Intelligence (AI) tools in the creation of this article.

Acknowledgments

This research was supported by the National Natural Science Foundation of China (No. 11971275) and the Natural Science Foundation of Shandong Province, China (No. ZR2019MA048).

Conflict of interests

The authors declare that they have no competing interests.

References

1. J. Hartog, Forced vibrations with combined viscous and coulomb damping, *Phil. Mag.*, **9** (1930), 801–817.
2. B. F. Feeny, F. C. Moon, Bifurcation sequences of a coulomb friction oscillator, *Nonlinear Dyn.*, **4** (1993), 25–37. https://doi.org/10.1007/bf00047119
3. K. Popp, N. Hinrichs, M. Oestreich, Dynamical behaviour of a friction oscillator with simultaneous self and external excitation, *Sadhana*, **20** (1995), 627–654. https://doi.org/10.1007/BF02823210
4. U. Galvanetto, Dynamics of a three DOF mechanical system with dry friction, *Phys. Lett. A*, **248** (1998), 57–66. https://doi.org/10.1016/S0375-9601(98)00644-6
5. U. Galvanetto, Non-linear dynamics of multiple friction oscillators, *Comput. Methods Appl. Mech. Engrg.*, **178** (1999), 291–306. https://doi.org/10.1016/S0045-7825(99)00021-3
6. J. Alvarez, I. Orlov, L. Acho, An invariance principle for discontinuous dynamic systems with application to a coulomb friction oscillator, *J. Dyn. Sys. Meas. Control*, **122** (2000), 317–322. https://doi.org/10.1115/1.1317229
7. J. J. Sinou, F. Thouverez, L. Jezequel, O. Dereure, G. B. Mazet, Friction induced vibration for an aircraft brake system-part 2: nonlinear dynamics, *Int. J. Mech. Sci.*, **48** (2006), 555–567.
8. R. Martinez, J. Alvarez, A controller for 2-DOF underactuated mechanical systems with discontinuous friction, *Nonlinear Dyn.*, **53** (2007), 191–200. https://doi.org/10.1007/s11071-007-9307-1
9. X. P. Li, C. S. Liu, J. Huang, B. C. Wen, Theoretical research and experiment of vibration friction on vibratory compaction experiment system, *Adv. Mat. Res.*, **118** (2010), 414–418.
10. Q. H. Li, Y. M. Chen, Z.Y. Qin, Existence of stick-slip periodic solutions in a dry friction oscillator, *Chin. Phys. Lett.*, **28** (2011), 030502. https://doi.org/10.1088/0256-307X/28/3/030502
11. H. B. Fang, X. Jian, Dynamics of a three-module vibration-driven system with non-symmetric coulomb's dry friction, *Multibody Syst. Dyn.*, **27** (2012), 455–485. https://doi.org/10.1007/s11044-012-9304-0
12. Y. Liu, L. H. Wen, Adaptive vibration control for system with friction damping, *Adv. Mat. Res.*, **403** (2012), 138–144.
13. N. A. Saadabad, H. Moradi, G. Vossoughi, Dynamic modeling, optimized design, and fabrication of a 2-DOF piezo-actuated stick-slip mobile microrobot, *Mech. Mach. Theory*, **133** (2019), 514–530. https://doi.org/10.1016/j.mechmachtheory.2018.11.025
14. B. Balachandran, A. H. Nayfeh, Nonlinear motions of beam-mass structure, *Nonlinear Dyn.*, **1** (1990), 39–61.
15. B. Balachandran, M. X. Zhao, Y. Y. Li, Dynamics of elastic structures subjected to impact excitations, In *IUTAM Symposium on New Applications of Nonlinear and Chaotic Dynamics in Mechanics*, Springer, 1999, 263–272.
16. B. Balachandran, Dynamics of an elastic structure excited by harmonic and aharmonic impactor motions, *J. Vib. Control*, **9** (2003), 265–279.

17. J. Zhang, L. S. Fan, Z. Chao, R. Pfeffer, D. Qi, Dynamic behavior of collision of elastic spheres in viscous fluids, *Powder Technol.*, **106** (1999), 98–109. https://doi.org/10.1016/S0032-5910(99)00053-4

18. Z. Liu, Z. Li, B. Cao, Collision detection and response of dynamic cloth simulation in virtual environment, *J. Syst. Simul.*, **19** (2007), 1497–1499. https://doi.org/10.1360/jos182955

19. Z. H. Tian, L. Zhao, Y. Jia, Research of dynamic collision detection algorithm based on entity behaviors, *J. Syst. Simul.*, **21** (2009), 1380–1383. https://doi.org/10.1360/972009-1549

20. Q. W. Ma, L. N. Yun, S. P. Ma, H. T. Wang, Experimental study on dynamic collision characteristics of concrete, *Adv. Mat. Res.*, **150** (2011), 937–940.

21. R. R. Aguiar, H. I. Weber, Mathematical modeling and experimental investigation of an embedded vibro-impact system, *Nonlinear Dyn.*, **65** (2011), 317–334. https://doi.org/10.1007/s11071-010-9894-0

22. A. Bichri, M. Belhaq, J. Perret-Liaudet, Control of vibroimpact dynamics of a single-sided hertzian contact forced oscillator, *Nonlinear Dyn.*, **63** (2011), 51–60. https://doi.org/10.1007/s11071-010-9784-5

23. A. Afsharfard, Application of nonlinear magnetic vibro-impact vibration suppressor and energy harvester, *Mech. Syst. Signal Pr.*, **98** (2018), 371–381. https://doi.org/10.1016/j.ymssp.2017.05.010

24. T. Li, C. H. Lamarque, S. Seguy, A. Berlioz, Chaotic characteristic of a linear oscillator coupled with vibro-impact nonlinear energy sink, *Nonlinear Dyn.*, **91** (2018), 2319–2330.

25. T. C. Harris, Periodic motions of arbitrarily long periods in non-linear spring-mass systems, *Int. J. Nonlinear Mech.*, **5** (1970), 491–500. https://doi.org/10.1016/0020-7462(70)90010-7

26. D. H. Campen, E. Vorst, J. Spek, A. Kraker, Dynamics of a multi-DOF beam system with discontinuous support, *Nonlinear Dyn.*, **8** (1995), 453–466. https://doi.org/10.1007/BF00045708

27. E. Vorst, D. Campen, A. D. Kraker, R. Fey, Periodic solutions of a multi-DOF beam system with impact, *J. Sound Vib.*, **192** (1996), 913–925.

28. S. Natsiavas, Stability of piecewise linear oscillators with viscous and dry friction damping, *J. Sound Vib.*, **217** (1998), 507–522. https://doi.org/10.1006/jsvi.1998.1768

29. S. Natsiavas, G. Verros, Dynamics of oscillators with strongly nonlinear asymmetric damping, *Nonlinear Dyn.*, **20** (1999), 221–246. https://doi.org/10.1023/A:1008398813070

30. O. Janin, C.H. Lamarque, Stability of singular periodic motions in a vibro-impact oscillator, *Nonlinear Dyn.*, **28** (2002), 231–241.

31. M. Arsenault, C.M. Gosselin, Kinematic, static and dynamic analysis of a planar 2-DOF tensegrity mechanism, *Mech. Mach. Theory*, **41** (2006), 1072–1089. https://doi.org/10.1016/j.mechmachtheory.2005.10.014

32. A. Luo, B.C. Gegg, An analytical prediction of sliding motions along discontinuous boundary in non-smooth dynamical systems, *Nonlinear Dyn.*, **49** (2007), 401–424. https://doi.org/10.1007/s11071-006-9130-0

33. G. W. Luo, X. H. Lv, X. F. Zhu, Dynamics of vibro-impact mechanical systems with large dissipation, *Int. J. Mech. Sci.*, **50** (2008), 214–232. https://doi.org/10.1016/j.ijmecsci.2007.07.001

34. M. Pascal, Dynamics of coupled oscillators excited by dry friction, *J. Comput. Nonlinear Dyn.*, **3** (2008).

35. A. Luo, J. Huang, Discontinuous dynamics of a non-linear, self-excited, friction-induced, periodically forced oscillator, *Nonlinear Anal.*, **13** (2012), 241–257. https://doi.org/10.1016/j.nonrwa.2011.07.030

36. L. A. Igumnov, V. S. Metrikin, M. V. Zaythev, Dynamics of a frictional system, accounting for hereditary-type friction and the mobility of the vibration limiter, *J. Phys.*, **1141** (2018), 012043. https://doi.org/10.1088/1742-6596/1141/1/012043

37. S. Xing, A. Luo, On possible infinite bifurcation trees of period-3 motions to chaos in a time-delayed, twin-well duffing oscillator, *Int. J. Dyn. Control*, **6** (2018), 1429–1464.

38. A. Filippov, Differential equations with discontinuous right-hand side, *Amer. Math. Soc. Transl.*, **2** (1964), 199–231.

39. A. Filippov, *Differential equations with discontinuous righthand sides,* Dordrecht: Kluwer Academic Publishers, 1988.

40. A. Luo, A theory for non-smooth dynamic systems on the connectable domains, *Commun. Nonlinear Sci. Numer. Simul.*, **10** (2005), 1–55. https://doi.org/10.1016/j.cnsns.2004.04.004

41. A. Luo, B.C. Gegg, Periodic motions in a periodically forced oscillator moving on an oscillating belt with dry friction, *J. Comput. Nonlinear Dyn.*, **1** (2005), 212–220. https://doi.org/10.1115/1.2198874

42. A. Luo, Flow switching bifurcations on the separation boundary in discontinuous dynamical systems with flow barriers, *Proc. Inst. Mech. Eng*, **221** (2007), 475–495. https://doi.org/10.1243/14644193JMBD42

43. A. Luo, On flow switching bifurcations in discontinuous dynamical systems, *Commun. Nonlinear Sci.*, **12** (2007), 100–116. https://doi.org/10.1016/j.cnsns.2006.01.010

44. A. Luo, A theory for flow switchability in discontinuous dynamical systems, *Nonlinear Anal.*, **2** (2008), 1030–1061. https://doi.org/10.1016/j.nahs.2008.07.003

45. A. Luo, *Discontinuous dynamical systems on time-varying domains*, Beijing: Higher Education Press, 2009.

46. A. Luo, T. T. Mao, Analytical conditions for motion switchability in a 2-DOF friction-induced oscillator moving on two constant speed belts, *Can. Appl. Math. Q.*, **127** (2009), 201–242.

47. A. Luo, *Discontinuous dynamical systems*, Beijing: Higher Education Press, 2012.

48. A. Luo, Flow barriers and switchability, *Discontin. Dyn. Syst.*, 2012, 165–258.

49. X. Fu, Y. Zhang, Stick motions and grazing flows in an inclined impact oscillator, *Chaos Solitons Fract.*, **76** (2015), 218–230. https://doi.org/10.1016/j.chaos.2015.04.005

50. J. Huang, A. Luo, Complex dynamics of bouncing motions at boundaries and corners in a discontinuous dynamical system, *ASME J. Comput. Nonlinear Dyn.*, **12** (2017), 61011–61014. https://doi.org/10.1115/1.4036518

51. J. Fan, X. Shan, S. Li, Analysis of dynamical behaviors of a friction-induced oscillator with switching control law, *Chaos Solitons Fract.*, **103** (2017), 513–531. https://doi.org/10.1016/j.chaos.2017.07.009

52. S. Chen, J. Fan, T. Liu, On discontinuous dynamics of a 2-DOF friction-influenced oscillator with multiple elastic constraints, *Int. J. Nonlinear Mech.*, **110** (2019), 131–150. https://doi.org/10.1016/j.ijnonlinmec.2018.12.004

53. M. Gao, J. Fan, Analysis of dynamical behaviors of a 2-DOF friction oscillator with elastic impacts and negative feedbacks, *Nonlinear Dyn.*, **102** (2020), 1–34. https://doi.org/10.1007/s11071-020-05904-z

54. Y. Peng, J. Fan, M. Gao, J. Li, Discontinuous dynamics of an asymmetric 2-DOF friction oscillator with elastic and rigid impacts, *Chaos Solitons Fract.*, **150** (2021), 111195. https://doi.org/10.1016/j.chaos.2021.111195

55. W. Li, L. Huang, J. Wang, Global asymptotical stability and sliding bifurcation analysis of a general Filippov-type predator-prey model with a refuge, *Appl. Math. Comput.*, **405** (2021), 126263. https://doi.org/10.1016/j.amc.2021.126263